American Psychological Association

Behavioral Neuroscience

0735-7044/18/$12.00

2018, Vol. 132, No. 5, 339–355
http://dx.doi.org/10.1037/bne0000278

Converging Meta-Analytic and Connectomic Evidence for Functional Subregions Within the Human Retrosplenial Region

Elizabeth R. Chrastil
Boston University and University of California, Santa Barbara

Sean M. Tobyne, Rachel K. Nauer, Allen E. Chang, and Chantal E. Stern
Boston University

Interest in the retrosplenial cortex (RSC) has surged in recent years, as this region has been implicated in a range of cognitive processes. Previously reported anatomical and functional definitions of the human RSC encompass a larger area than expected from underlying cytoarchitectonic profiles. Here, we used a large-scale, unbiased, and data-driven approach combining functional MRI meta-analysis and resting-state functional connectivity (rsFC) methods to test the nature of this heterogeneity. The automated toolset Neurosynth was used to conduct meta-analyses in order to (a) identify heterogeneous areas in the retrosplenial region (RS region) associated with one or more cognitive domains, and (b) contrast the activation profiles related to these domains. These analyses yielded several functional subregions across the RS region, highlighting differences between anterior RS regions associated with episodic memory and posterior RS regions in the parietal-occipital sulcus associated with scenes and navigation. These regions were subsequently used as seeds to conduct whole brain rsFC analyses using data from the Human Connectome Project. In support of the meta-analysis findings, rsFC revealed divergent connectivity profiles, with anterior regions demonstrating connectivity to the default mode network (DMN) and posterior regions demonstrating connectivity to visual regions. Anterior RS regions and the parietal-occipital sulcus connected to different subnetworks of the DMN. This convergent evidence supports the conclusion that the broad cortical RS region incorporating both anatomical and functional RSC consists of functionally heterogeneous subregions. This study combines two large databases to provide a novel methodological blueprint for understanding brain function in the RS region and beyond.

Keywords: navigation, episodic memory, scene perception, imagery, functional connectivity

Supplemental materials: http://dx.doi.org/10.1037/bne0000278.supp

The retrosplenial cortex (RSC), located at the confluence of the limbic, parietal, and visual cortical areas, has been associated with many diverse functions, sparking intense debate regarding its role in cognition and behavior. Functional MRI (fMRI) studies have implicated both the anatomical RSC as well as adjacent regions in scene perception (Epstein & Higgins, 2007; Park, Intraub, Yi, Widders, & Chun, 2007; Summerfield, Hassabis, & Maguire, 2010), spatial navigation (Auger, Mullally, & Maguire, 2012; Chrastil, Sherrill, Hasselmo, & Stern, 2015; Sherrill et al., 2013; Wolbers & Büchel, 2005), episodic and autobiographical memory (Steinvorth, Corkin, & Halgren, 2006; Summerfield, Hassabis, & Maguire, 2009; Vincent et al., 2006), head direction (Baumann &

Elizabeth R. Chrastil, Department of Psychological and Brain Sciences, Center for Memory and Brain, Boston University, and Department of Geography, University of California, Santa Barbara; Sean M. Tobyne, Department of Psychological and Brain Sciences, Center for Memory and Brain, Kilachand Center for Integrated Life Sciences and Engineering, and Graduate Program for Neuroscience, Boston University; Rachel K. Nauer and Allen E. Chang, Department of Psychological and Brain Sciences, Center for Memory and Brain, Kilachand Center for Integrated Life Sciences and Engineering, and Brain, Behavior, and Cognition Program, Boston University; Chantal E. Stern, Department of Psychological and Brain Sciences, Center for Memory and Brain, Kilachand Center for Integrated Life Sciences and Engineering, Boston University.

Elizabeth R. Chrastil and Sean M. Tobyne contributed equally to this work. Elizabeth R. Chrastil, Sean M. Tobyne, Rachel K. Nauer, and Allen E. Chang designed the research; Elizabeth R. Chrastil, Sean M. Tobyne, Rachel K. Nauer, and Allen E. Chang performed the research; Elizabeth R. Chrastil, Sean M. Tobyne, Rachel K. Nauer, and Allen E. Chang analyzed the data; Elizabeth R. Chrastil, Sean M. Tobyne, and Chantal E. Stern wrote the article; and Chantal E. Stern oversaw the project.

This work was supported by the Office of Naval Research MURI N00014-10-1-0936 and MURI N00014-16-1-2832. We thank David Osher for his assistance in data preprocessing and conducting the PubMed keyword scrape. We thank Yiren Ren for her assistance with the search space and manual meta-analysis. We thank Tal Yarkoni for his assistance using Neurosynth. We thank James Brissenden for assistance with the hierarchical cluster analysis. We thank David Somers for his helpful comments. Portions of this work were presented at the Society for Neuroscience annual meeting (2016), San Diego, California, and the International Conference on Learning and Memory (2018), Huntington Beach, California.

Correspondence concerning this article should be addressed to Elizabeth R. Chrastil, Department of Geography, University of California, Santa Barbara, 1832 Ellison Hall, Santa Barbara, CA 93106-4060. E-mail: chrastil@ucsb.edu

Mattingley, 2010; Marchette, Vass, Ryan, & Epstein, 2014; Shine, Valdés-Herrera, Hegarty, & Wolbers, 2016), pain and emotional processing (Kucyi et al., 2014; Luo et al., 2014), and mental imagery (Boccia et al., 2015; Summerfield et al., 2009; see Chrastil, 2018, pp. 317–338, for review). The sheer number of functions ascribed to the human RSC may be a result of varying locations across the medial parietal and occipital lobes that have been identified as RSC in previous studies (see Figure 1). Previous research on the RSC and its function has largely viewed the region through the lens of a particular cognitive domain (e.g., episodic memory or navigation). Although these domain-specific approaches have yielded considerable insight into RSC function, they have also led to difficulty in synthesizing a broader understanding of the region across domains.

A second complication in determining RSC function, at least in humans, has been the lack of consensus on its anatomical, histological, and functional boundaries; fMRI studies refer to this area as the *retrosplenial cortex*, *complex*, *area*, or *region*. Although the splenium of the corpus callosum and the parietal-occipital sulcus (POS) provide respective anterior and posterior anatomical boundaries of the RSC (Kobayashi & Amaral, 2000; Vann, Aggleton, & Maguire, 2009), there are no clear anatomical boundaries with the precuneus, parahippocampal cortex (PHC), or posterior cingulate cortex (Kobayashi & Amaral, 2000; Pruessner et al., 2002). Furthermore, subdivisions of higher order cortical regions based upon anatomical definitions or folding patterns provide poor alignment across subjects (Amunts, Schleicher, & Zilles, 2007; Robinson et al., 2014). Histological studies have shown that granular cortex is located in Brodmann areas (BAs) 29a to 29c, whereas dysgranular cortex is found in BA30 (Figure 1B; Kobayashi & Amaral, 2000; Vann et al., 2009; Vogt, Vogt, Perl, & Hof, 2001). BA30v in the depths of the anterior calcarine sulcus and BA23 in the nearby posterior cingulate are often included in discussions of the greater RSC (Kobayashi & Amaral, 2000), although not without debate (Vann et al., 2009). Unfortunately, these cytoarchitectonic subdivisions cannot typically be resolved from standard-resolution MRI, limiting the utility of these boundaries for in vivo human imaging (although see Fischl et al., 2008). Employing functional definitions of the RSC can circumvent many of these problems, but they are less useful for generalizing across studies because they restrict interpretation to an a priori function. For scene perception, these tasks typically recruit regions posterior to BA29 and BA30 and include the POS, lingual gyrus, and calcarine sulcus (Epstein & Kanwisher, 1998; Marchette et al., 2014; Park & Chun, 2009; Silson, Steel, & Baker, 2016; Vass & Epstein, 2013). Together, these areas are often defined more broadly as the *retrosplenial complex* (Epstein, 2008), further blurring the definition of the RSC with adjacent, seemingly functionally distinct, cortex.

Because of the lack of consensus regarding RSC boundaries between these three methodologies, in our meta-analysis, we use the term *retrosplenial region* (*RS region*) to refer to a broad area of cortex encompassing both the anatomical RS cortex as well as

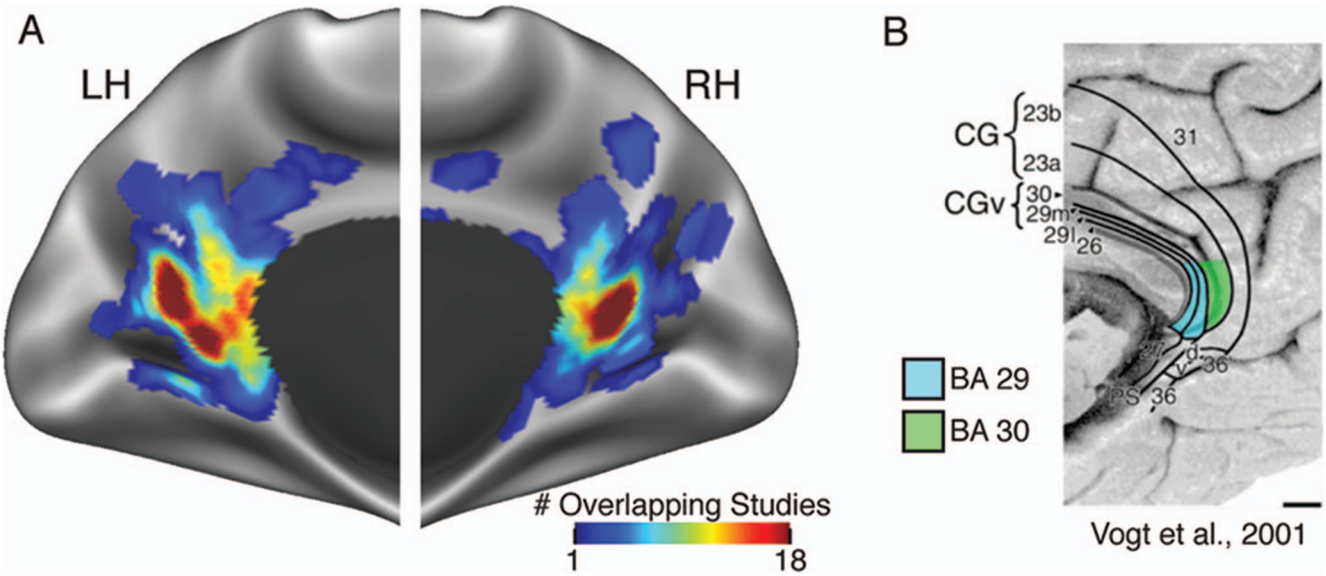

Figure 1. (A) Reported fMRI peak activation coordinates for studies associated with the terms *retrosplenial cortex*, *complex*, *area*, or *region*. The frequency of a coordinate reported as a significant retrosplenial activation in the 96 studies that make up the multi-level kernel density analysis manual meta-analysis (Wager et al., 2007, 2009). The term *retrosplenial* is used to refer to a large swath of cortical area that spans several anatomical regions, highlighting the variability and lack of consensus in defining retrosplenial cortex. Areas of meta-analysis activation are shown in dark gray, with brighter spots having higher *z*-scores. See also Supplemental Table 1 of the online supplemental materials. (B) Illustration of approximate location of histologically defined Brodmann Areas 29 (blue [dark gray]) and 30 (green [light gray]). Adapted from "Cytology of Human Caudomedial Cingulate, Retrosplenial, and Caudal Parahippocampal Cortices," by B. A. Vogt, L. J. Vogt, D. P. Perl, and P. R. Hof, 2001, *Journal of Comparative Neurology, 438*, p. 372. Copyright (2001) by Wiley Publishing. Adapted with permission. See the online article for the color version of this figure.

adjacent areas highlighted in Figure 1A. It is important to understand that this region extends well beyond the boundaries of the RSC, as defined by animal and histological studies, to include portions of the posterior cingulate, precuneus, parietal-occipital sulcus, calcarine sulcus, and lingual gyrus. These regions have been included in prior functional definitions of the RSC and were identified in our meta-analyses as having RS region coordinates. Mapping the terminology used in human fMRI studies onto the histologically defined areas is complicated. Where appropriate, we included both anatomical labels (e.g., parietal-occipital sulcus) and functional labels (e.g., posterior RS region) to facilitate the mapping between anatomical and functional approaches.

The primary goal of this study was to test the hypothesis that the human RS region is functionally heterogeneous and possesses subregions of function, similar to the functional gradient observed in rodents (Pothuizen, Davies, Albasser, Aggleton, & Vann, 2009). In order to test this hypothesis, we circumvented the issues of domain bias and variable definitions of the RSC by using an unbiased, wide-lens, data-driven approach combining fMRI meta-analysis and resting-state functional connectivity (rsFC). This approach leveraged the vast array of past research on the RSC while minimizing the potential for perspectives that are biased a priori for certain cognitive domains. Using these data-driven methods, we (a) provide strong evidence for functional subregions across the RS region, and (b) establish an approach demonstrating the utility of combining meta-analysis of published fMRI results and rsFC from large-scale databases for understanding brain function in the RS region and throughout the brain.

Method

The primary analyses in this study were conducted using Neurosynth (Yarkoni, Poldrack, Nichols, Van Essen, & Wager, 2011), an online meta-analysis tool set consisting of over 11,000 fMRI and rsFC studies that produces automated meta-analyses of terms, general topic areas, custom groupings of publications, and searches by coordinate locations. Using Neurosynth, we automatically selected publications significantly more likely to be associated with the search term *retrosplenial* and matched them to their most commonly reported cognitive domains. We then used a series of domain-specific meta-analyses to localize RS regions associated with each cognitive domain and conducted meta-analytic contrasts between domains to establish uniquely recruited cortex. Results were confirmed with an additional manual meta-analysis (Wager, Lindquist, & Kaplan, 2007; Wager, Lindquist, Nichols, Kober, & Van Snellenberg, 2009). Regions of interest localized from the domain-specific meta-analyses were then used as seeds for rsFC analysis conducted on data drawn from the Human Connectome Project (HCP) database (van Essen et al., 2013), establishing the connectivity profiles of putative RS subregions and investigating how they cluster together. Finally, we developed a novel alternative approach by conducting a series of meta-analyses at each point of a grid across the entirety of the prospective RS region.

Retrosplenial fMRI Meta-Analysis

To identify specific studies associated with the term *retrosplenial*, we conducted an automated meta-analysis of 11,406 previously published studies using the Neurosynth platform (www.Neurosynth.org, accessed in January 2016; Yarkoni et al., 2011), yielding 101 relevant publications (see Supplemental Table 1 of the online supplemental materials). We determined the dominant cognitive constructs associated with the resultant publications by mining PubMed (www.ncbi.nlm.nih.gov/pubmed) XML metadata—limited to article titles, author-provided descriptors, and keywords. The frequency of a given term occurring within the aggregate XML metadata was calculated by entering the terms into an online histogram function (www.textfixer.com/tools/online-word-counter.php) that automatically removed common words such as *the* and *by*. To eliminate potential points of confusion (e.g., *temporal* could refer to time or the temporal lobe), we removed the spaces between words in the descriptors to provide context information. This process yielded 801 separate terms, over half of which appeared only once (see Supplemental Table 2 of the online supplemental materials).

Terms relating to demographics (e.g., *humans*, *female*, *adult*), specific brain regions (e.g., *parahippocampal gyrus*, *parietal lobe*), methodology (e.g., *neuropsychological tests*, *computer*, *reaction time*), and connector words (e.g., *between*, *role*, *versus*, *involvement*) were removed. We also removed terms for specific disorders, although we kept any associated cognitive terms (e.g., we kept *sleep* but not *sleep disorders* or *sleep apnea*). Four authors (ERC, SMT, RKN, and AEC) independently removed terms according to these criteria, with the goal of retaining only primary cognitive constructs. Interrater reliability was very high (intraclass correlation coefficient = 0.917), $F(777, 2331) = 45.154$, $p < .0001$. If three raters judged a term as included as a cognitive construct, it was retained. This reduction step resulted in 93 terms (see Supplemental Table 1). Terms with the same stems were then combined (e.g., *emotion* and *emotional*), as were terms with overlapping meanings (e.g., *spatial*, *navigation*, and *geographic mapping*). This final refinement step resulted in 12 terms: *emotion*, *executive function*, *haptic*, *imagery*, *language*, *learning*, *memory*, *navigation*, *scene*, *self*, *sleep*, and *vision*.

To assign each of the 101 publications to one of the 12 refined terms, we examined either the top 10 semantic loadings or all semantic loadings >0.2 (whichever set was larger) for "term frequency-inverse document frequency," a measure of normalized word frequency, within Neurosynth. We assigned each publication to a given category according to the magnitude of semantic loadings most closely associated with derived cognitive domains, with up to three domain assignments allowed per publication. If a category was assigned five or fewer articles (<5% of total articles), it was removed from further consideration. Seven cognitive domains met this selection criterion: *memory* (35 publications), *navigation* (20 publications), *scene processing* (14 publications), *emotion* (14 publications), *vision* (13 publications), *learning* (eight publications), and *imagery* (eight publications). Fifteen publications did not have sufficient loadings to catalog them into any category and were omitted from further analysis (see Supplemental Table 1). Although the derived *memory* term encompassed several declarative memory processes, such as semantic memory, the vast majority of *memory*-related publications concerned episodic and autobiographical process, and included no procedural or working memory processes. The results of this analysis are shown in Figure 2A and 2B.

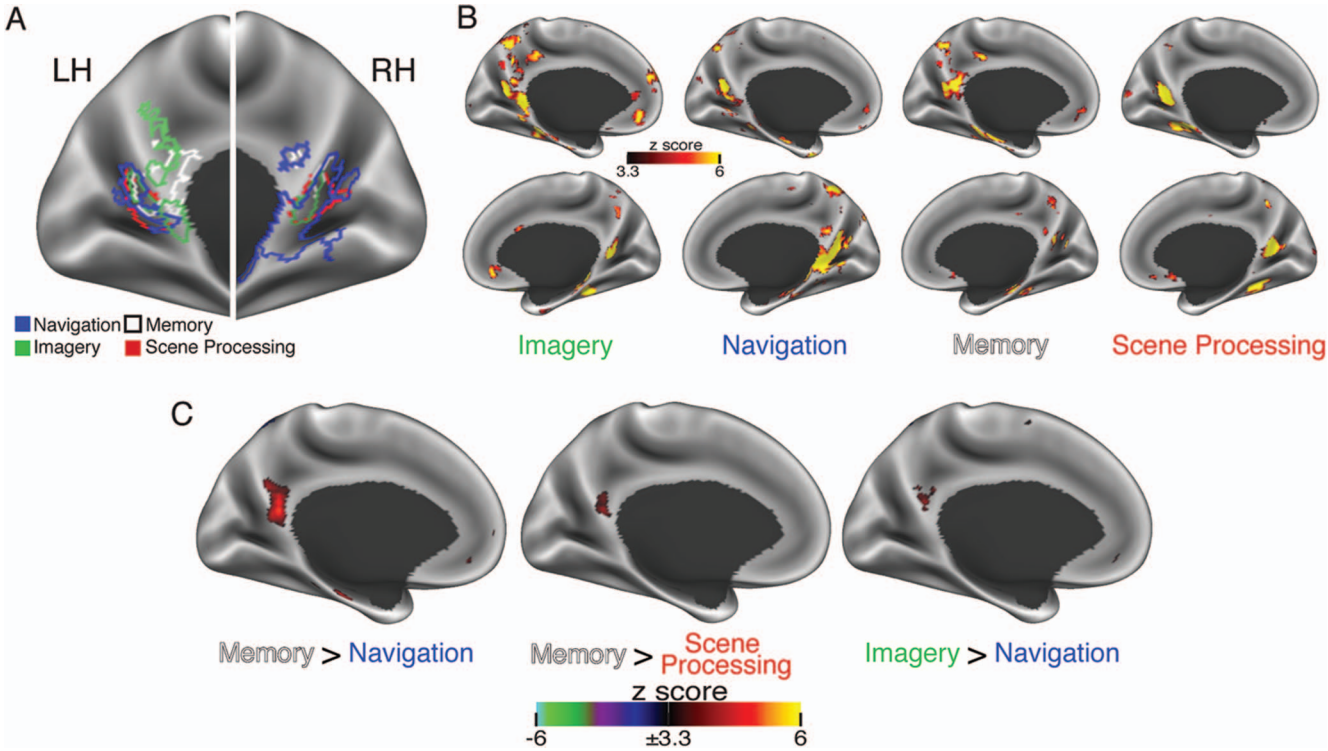

Figure 2. Primary meta-analysis results revealed overlapping and unique retrosplenial recruitment. (A) Regions of significant meta-analysis results from Neurosynth demonstrated strong overlap within the bilateral inferior parietal-occipital sulcus (POS) and unique associates within much of the remainder of the putative retrosplenial (RS) region (B) Individual meta-analysis results for the four dominant cognitive domains. These results are presented unmasked to display the full extent of the domains recruitment, even outside of the putative RS region. (C) Topic-based meta-analytic results generated by the contrast of *memory* > *navigation* (left), and *memory* > *scene processing* (center) revealed overlapping regions uniquely associated with *memory* located within the retrosplenial cortex. These regions share no anatomical overlap with the POS. Topic-based meta-analytic results generated by the contrast of *imagery* > *navigation* (right) revealed regions uniquely associated with *imagery* located within the retrosplenial cortex. The opposite contrasts (*navigation* > *memory*, *scene* > *memory*, and *navigation* > *imagery*) had no significant clusters. Color scale represents significant *z* score map output from Neurosynth resampled to the cortical surface, thresholded at $p < .001$, family-wise error corrected. See also Supplemental Figures 1, 2, and 3 and Supplemental Tables 1 and 2 of the online supplemental materials. POS = parietal-occipital sulcus. See the online article for the color version of this figure.

Topic-Based Meta-Analytic Contrasts of Cognitive Domains

We refined the results of our primary meta-analysis by leveraging the extensive breadth of information encapsulated by the Neurosynth database. Instead of focusing on *retrosplenial* as a search term, we targeted the derived cognitive domains. The 200-topic list was chosen to conduct topic-based meta-analysis (see Poldrack et al., 2012; Yarkoni et al., 2011, for details about the topic-based meta-analyses) to examine the extent of RS activation revealed by the four main results of interest from the primary retrosplenial meta-analysis: *episodic memory*, *navigation*, *scene perception*, and *imagery*. Meta-analysis results for individual topics are visible at http://neurosynth.org/analyses/topics/v4-topics-200 (Topic #3, 25, 48, and 151). The number of publications associated with each topic was as follows: *episodic memory* (314 publications), *navigation* (265 publications), *scene perception* (189 publications), and *imagery* (206 publications).

We then performed meta-analytic contrasts (Core Neurosynth Tools; https://github.com/neurosynth/neurosynth) of reported activation for each of the four primary results of the meta-analysis: *episodic memory*, *navigation*, *scene perception*, and *imagery*. These contrasts were used to localize significantly greater activation in one meta-analysis compared with another. Six individual contrasts of the four topics were conducted using the 200-topic set. The contrasts were thresholded at $z > 3.3$ ($p < .001$, uncorrected). The results are shown in Figure 2C.

Manual Retrosplenial fMRI Meta-Analysis

For replication and reliability purposes, we conducted a manual meta-analysis outside of Neurosynth with the goal of incorporating articles that may not exist in the Neurosynth database. We conducted a manual meta-analysis using multi-level kernel density analysis (MKDA; http://wagerlab.colorado.edu/tools; Wager et al., 2007, 2009). MKDA compares the raw proportion of studies

reporting activation near a given voxel or coordinate with the amount expected by chance. The search string "retrosplenial" AND "fmri" AND "human" was entered into PubMed, returning 308 publications. Publications were manually searched for reported coordinates, cluster size, and *t* or *z* values for peak activations, and the number of participants for each study. Coordinates that fell within a broad RS region, which were generally listed as "retrosplenial" but sometimes as "posterior cingulate," "parietal-occipital sulcus," or "posterior parietal," were selected for inclusion. We excluded publications that did not supply coordinates for the peak or center-of-mass of significant clusters, utilized animal models, or examined clinical populations without conducting separate analyses on control subjects. Of the 308 publications originally gleaned from PubMed, 96 passed these criteria. A total of 50 publications overlapped between the manual and Neurosynth publication lists (see Supplemental Table 1). Publications were manually categorized into the 12 cognitive domains, derived from the initial cognitive domains determined from the earlier Neurosynth analysis, based on the experimental details of each study. Two authors (ERC and AEC) independently categorized the publications into domains, and differences were reconciled into a final list. Each publication could be categorized into up to three cognitive domains. Similar to the Neurosynth meta-analysis, any category with five or fewer assigned articles was removed. This refinement resulted in seven cognitive domains that met this selection criterion: *memory* (35 publications), *navigation* (26 publications), *scene processing* (18 publications), *self* (nine publications), *emotion* (eight publications), *imagery* (eight publications), and *vision* (six publications). Each domain-specific subgroup was then subjected to separate meta-analyses using MKDA. We report results for clusters that passed the "height" threshold, which is the strictest significance threshold available in MKDA ($p < .001$ level, FEW corrected, 10,000 Monte Carlo simulations). The results are shown in Figure 3.

Cognitive Domain Retrosplenial Grid Search

To identify cognitive domains associated with the RS region irrespective of the term *retrosplenial* or our derived cognitive domains, we used Neurosynth's "Locations" function. This function returns studies reporting activation within a variable radius of the desired Montreal Neurological Institute (MNI) coordinate and provides reverse inference *z* scores for terms associated with that location. This process "flips" the meta-analysis process; instead of entering cognitive domains and finding the associated locations, we entered locations and found the associated cognitive domains. We sampled a 3D grid of 3-mm-radius spherical neighborhoods at 5-mm intervals from the following MNI coordinates: X = −20 to +20, Y = −42 to −72, Z = −2 to +28. *Z* scores for terms that were above the uncorrected $p < .001$ level ($z > 3.3$) were collected from each grid point. Similar to the initial meta-analysis, terms pertaining to demographics, specific brain regions, specific brain disorders, methodology, and connector words were removed, and terms with overlapping meaning were combined. This refinement resulted in a final list of 30 possible terms associated with a broadly defined retrosplenial search space (see Supplemental Table 3 of the online supplemental materials). This list was limited to the eight most frequently appearing terms by truncating the list at

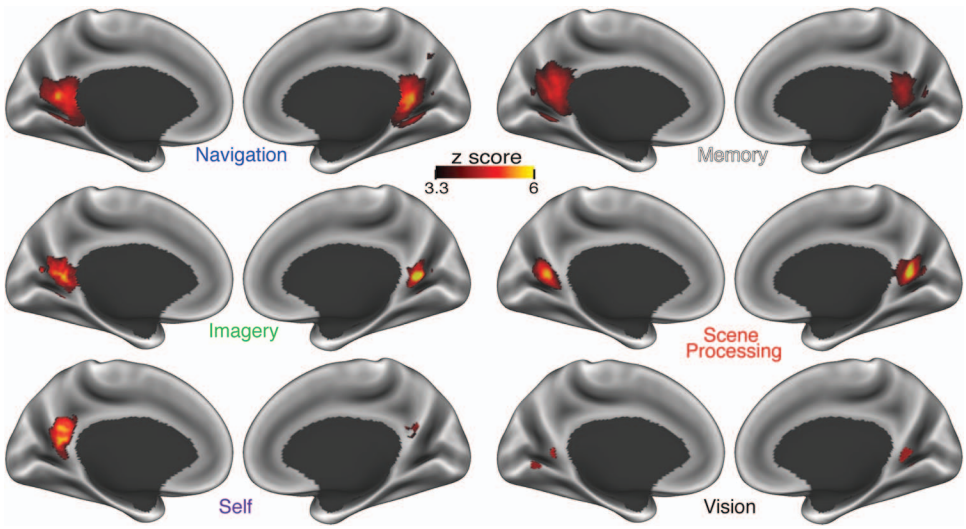

Figure 3. Results from the manual meta-analysis using MKDA. *Navigation*, *imagery*, and *scene processing* all displayed strong overlap in the POS; however, only *memory* and *navigation* overlapped within the anatomical RSC. *Self* was largely found in anterior RS regions and extended further into the precuneus than other domains. Little evidence was found for *vision* as a significant domain. *Emotion* did not return any significant voxels and is not shown. The minimum *p* value from the MKDA analysis shows the clusters for which the proportion of contrast activation were greater than would be expected by chance across the whole brain level at $p < .001$, family-wise error corrected to $p < .05$, 10,000 Monte Carlo simulations. There was no maximum *p* value in this range; for illustration purposes, the maximum shown here multiples this threshold by 2.5. See also Supplemental Table 1 of the online supplemental materials. MKDA = multi-level kernel density analysis; POS = parietal-occipital sulcus; RSC = retrosplenial cortex. See the online article for the color version of this figure.

a clear drop-off (>40%) in word frequency. The final eight topics included *memory* (252 appearances), *navigation* (100 appearances), *scene* (60 appearances), *vision* (54 appearances), *self* (44 appearances), *emotion* (41 appearances), *imagery* (38 appearances), and *theory of mind* (35 appearances). Following the grid search and data scrubbing, each locus was assigned to a category using three strategies: (a) a winner-take-all system based on maximal z score to indicate which cognitive domain was represented at each location in the RS region; (b) combinations of *memory*, *navigation*, and *scenes* (ignoring all other terms) to evaluate neighborhoods against the most commonly attributed RS region functions; and (c) combinations of *memory*, *self*, and *theory of mind* (ignoring all other terms) to evaluate the novel emergence of *self* and *theory of mind* from these meta-analytic results.

Of the 441 grid points in the search space, 85 had no loadings with any of the eight cognitive domains. Of the remaining 356 grid points, 196 had only one loading, but 160 of the grid points were associated with multiple terms (Supplemental Table 3). Thus, the second two strategies were derived from overlap of the top three terms crossing the z threshold at a given grid point. The combinations of *memory* and *navigation* (13 appearances), *memory* and *scenes* (10 appearances), *memory* and *self* (11 appearances), *memory* and *theory of mind* (11 appearances), and the three-way combinations of *memory*, *navigation*, and *scenes* (27 appearances), and *memory*, *self*, and *theory of mind* (13 appearances) appeared most frequently in this analysis. We then counted when the terms of interest crossed the z threshold for all grid points, regardless of rank order.

Following the labeling of each grid point, the volumes were iteratively dilated by 5 mm to fill the space between grid points using nearest-neighbor interpolation. The volumes were then resampled to the fs_LR cortical surfaces (an HCP-specific version of FreeSurfer's fsaverage standard space with left and right hemispheres aligned) using Connectome Workbench's "-volume-to-surface-mapping" command and the "-enclosing" algorithm. The results are shown in Figure 4.

Resting State Functional Connectivity Analyses

Human Connectome Project data set. Publicly available MRI data acquired as part of the HCP (www.humanconnectome.org) and supported by the WU-Minn HCP Consortium were used for all rsFC analyses (van Essen et al., 2013). All participants in the HCP data set gave informed consent for the study, in compliance with the ethics committee of Washington University in St. Louis and the University of Minnesota. Pulse sequences and acquisition protocols for the HCP dataset are detailed extensively elsewhere (Barch et al., 2013; Smith et al., 2013; Sotiropoulos et al., 2013; van Essen et al., 2013). Briefly, subjects underwent 2 days of scanning on the custom Siemens Connectome Skyra MRI scanner (Siemens, Erlangen, Germany) located at Washington University in St. Louis. Across the 2 days of scanning, high-resolution (0.7-mm isotropic voxel size) T1- and T2-weighted structural images and up to four rs-fMRI sequences (repetition time (TR)/echo time (TE) = 720/33.1 ms, flip angle = 52°, multiband factor = 8, 72 slices, 2 mm isotropic voxels, 1200 TRs) were acquired; rs-fMRI sequences were acquired in pairs of left-right and right-left phase encoding, one pair on each scan day. Preprocessed and denoised resting-state data for 100 unrelated participants were downloaded from http://db.humanconnectome.org (hereafter referred to as "HCP100") and used for functional connectivity analyses.

HCP100 resting-state preprocessing. Data from the HCP was preprocessed using a freely available set of pipelines (available at https://github.com/Washington-University/Pipelines) described as "minimally preprocessed" (MPP) data by the HCP—prior to being made available to the public (Glasser et al., 2013). This includes both spatial (gradient nonlinearity correction, motion correction, EPI readout distortion correction) and temporal (automated ICA denoising with Functional MRI of the Brain [FMRIB]'s ICA-based Xnoisefier [FIX]; Griffanti et al., 2014; Salimi-Khorshidi et al., 2014) artifact correction, high-pass filtering (0.0005-Hz cutoff), and nonlinear registration to fs_LR (a down-sampled HCP-specific version of FreeSurfer's fsaverage standard space with left and right hemispheres aligned) template space via the subjects' own reconstructed cortical surfaces. FIX has been shown to be effective in the removal of physiological- and/or motion-induced noise variance in rsfMRI data (Griffanti et al., 2014; Salimi-Khorshidi et al., 2014). Thus, regression of physiological parameters recorded during the scan (e.g., heart rate or breathing rate) were not explicitly regressed from the data. rsfMRI data that is processed through the HCP pipelines is referred to as MPP + FIX data to reflect the HCP pipelines that have been applied. We developed custom MATLAB functions to perform additional preprocessing steps on the MPP + FIX data, including, in order, linear interpolation across high-motion timepoints (>0.5 mm framewise displacement (Power et al., 2014), temporal filtering with a fourth-order Butterworth bandpass filter ($0.009 < f < 0.08$), censoring of high-motion time points by deletion and temporal denoising with mean "grayordinate" signal regression (i.e., all gray matter voxels/vertices; Burgess et al., 2016). Following the application of these preprocessing steps on individual rs-fMRI acquisitions, all four rs-fMRI acquisitions were separately temporally demeaned and then concatenated into a single file of 4800 TRs.

Region of interest definition. Reverse inference maps from the primary Neurosynth meta-analyses were used to define a set of regions of interest (ROIs) for rsFC analyses, yielding 18 seeds. Maps of the *emotion*, *memory*, *navigation*, *scene processing*, and *imagery* meta-analytic results were resampled to the fs_LR cortical surface using Connectome Workbench's "-volume-to-surface-mapping" command and employing the "-ribbon-constrained mapping" algorithm, which uses the white and pial surfaces within the mapping procedure. For each domain, clusters that passed the threshold ($z > 3.3$, $p < .001$, uncorrected) were designated as ROIs (results panel D). ROIs from the *emotion* domain were included with ROIs from the four primary domains of interest because they demonstrated a bilateral anterior-to-posterior progression of connectivity profile—warranting their examination in depth (see Figure 5). ROIs from the *vision* and *learning* domains were small (surface area of <50 mm^2), were located at the far extent of the putative RS region search space, or were present in only one hemisphere and were thus excluded from the resting-state analyses. We have made the ROIs publicly available through the Brain Atlas Library of Spatial Maps and Atlases (BALSA; Van Essen et al., 2017) host-

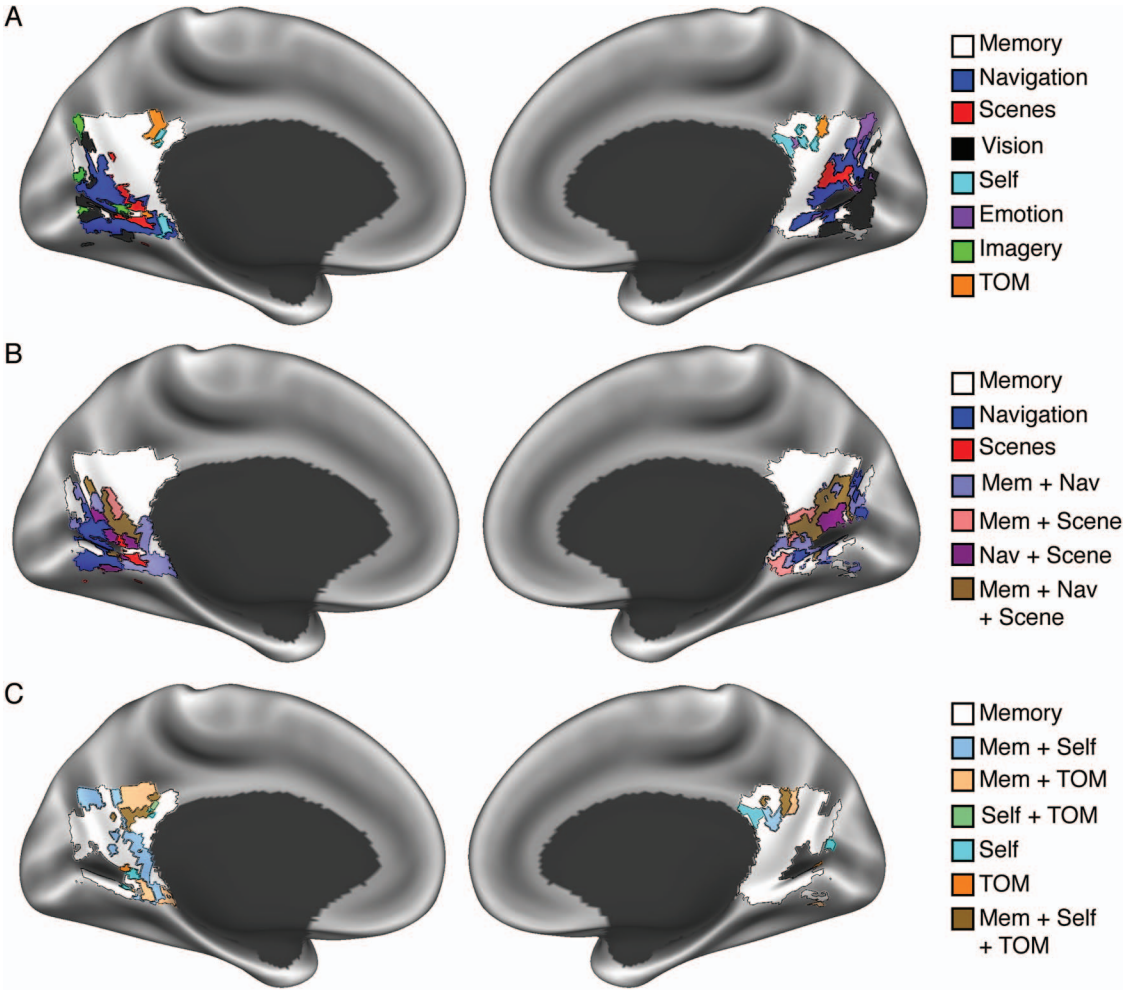

Figure 4. Results for primary and conjunction grid search meta-analyses. (A) Primary (winner-take-all), (B) *Memory/Navigation/Scenes* conjunction, and (C) *Memory/Self/Theory-of-Mind* conjunction grid search procedures together indicate a clear distinction between the anatomical RSC and POS, with *memory* providing a common binding element across much of the search space. *Z* scores for each location in the retrosplenial region were collected for terms that were above the uncorrected $p < .001$ level ($z > 3.3$). Clusters corresponding to derived cognitive domains are displayed within a generously defined RS region search space. Colors represent the most likely cognitive domain at each point. See Method for plotting procedures; see also Supplemental Figure 4 and Supplemental Table 3 of the online supplemental materials. RSC = retrosplenial cortex; POS = parietal-occipital sulcus. See the online article for the color version of this figure.

ing platform (https://balsa.wustl.edu/study/show/GgPq) to allow for open access to our materials for future replication.

Seed-to-whole-brain rsFC analyses. Whole-brain vertex-wise correlation maps were created for each HCP100 subject using each of the 18 seeds by first extracting rs-fMRI signal averaged over the vertices within that ROI and then calculating the Pearson correlation between all ipsilateral and contralateral cortical surface vertices. Correlation maps were normalized with Fisher's r-to-z transformation, concatenated and entered into a one-sample group-level analysis using FMRIB Software Library (FSL)'s Permutation Analysis of Linear Models (PALM) tool (Winkler, Ridgway, Webster, Smith, & Nichols, 2014; Winkler, Webster, Vidaurre, Nichols, & Smith, 2015), including correction for multiple comparisons ($p < .0001$, family-wise error [FWE] corrected, 10,000 sign-flips, cluster extent threshold $z = 3.1$). To quantify the differences between the correlation maps, we performed group-level contrasts between the correlation maps generated by each ROI. First, for each subject, we calculated the correlation between one ROI's correlation map and the correlation map generated by one of the other ipsilateral ROIs. We then conducted a one-sample *t* test on this correlation to test whether the correlation between correlation maps was significantly different from zero (Figure 5A). For correlation maps that were significantly correlated, we then performed a paired-sample group-level analysis using FSL's PALM tool (Winkler et al., 2014, 2015), including correction for multiple comparisons ($p < .0001$, FWE corrected, 10,000 sign-flips, cluster extent threshold $z = 3.1$), across the 100 subjects to identify

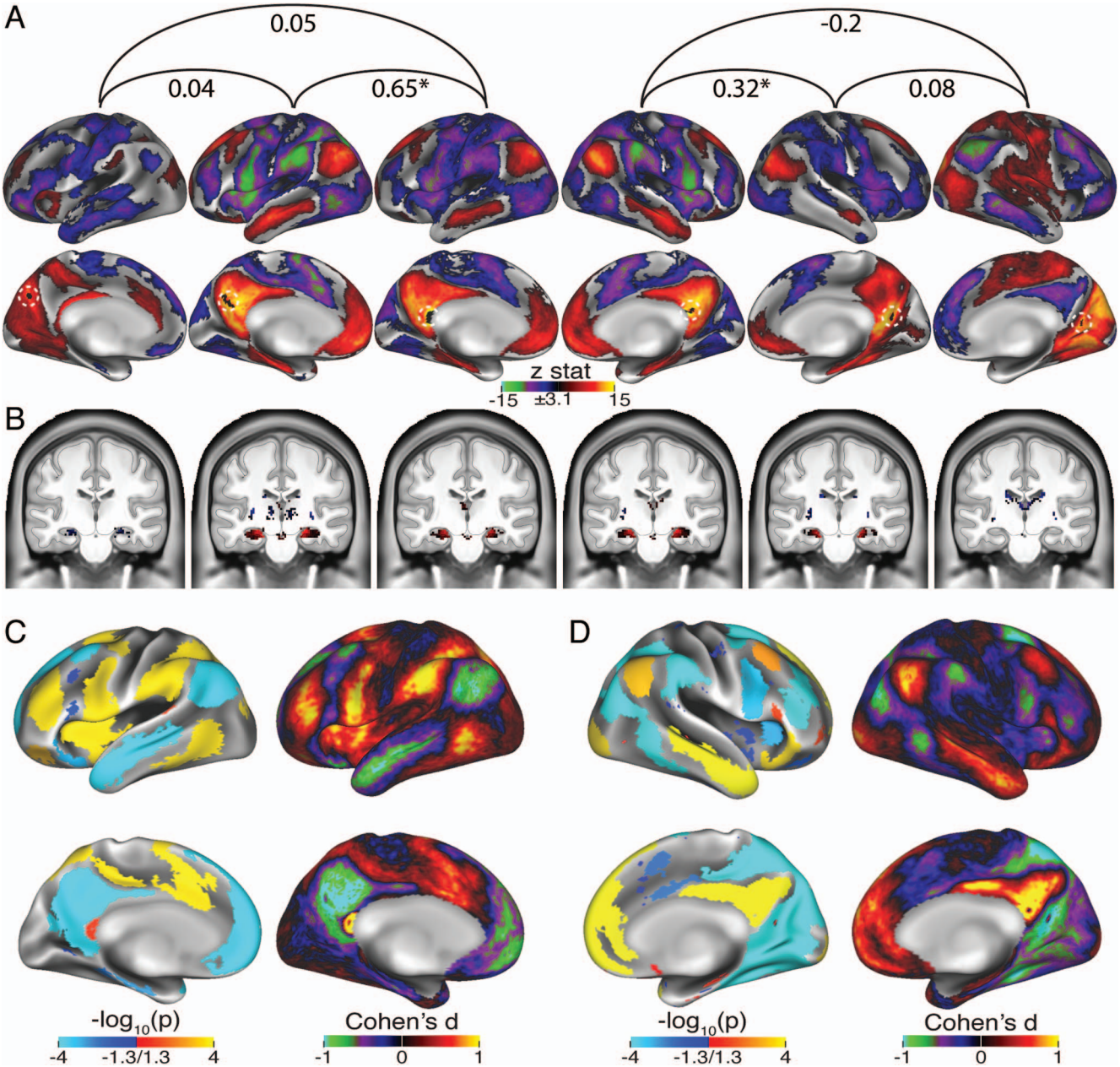

Figure 5. Functional connectivity profiles within HCP100 (n = 100 participants) data set vary across the retrosplenial (RS) region/POS. (A) regions of interest (ROIs) identified in the primary meta-analysis (black labels indicated by white dashed lines) produced patterns of functional connectivity that varied along a general anterior-to-posterior axis. Curved lines and associated values indicate the average correlation value, across subjects, between the whole brain correlation map generated by a given ROI and the whole brain correlation map for another ipsilateral ROI. These correlation values were entered into a one-sample t test against the null hypothesis that the correlation between maps was not significantly different from zero. * $p < .0001$. (B) Subcortical connectivity generated by the same ROIs revealed differences in subcortical connectivity, most prominently in the hippocampus. Black outlines indicate average midthickness of the fs_LR surfaces. Group-level analysis conducted with permutation analysis of linear models (PALM), $p < .0001$, family-wise error (FWE) corrected, 5,000 sign flips, cluster extent threshold $z = 3.1$. See also Supplemental Figures 5 and 6 of the online supplemental materials. (C) p values and effect size estimates from a paired-sample group-level analysis between the whole brain correlation maps generated from the more anterior left hemisphere ROI (third column) and the precuneus ROI (second column). Red area indicates the seed. (D) p values and effect size estimates from a paired-sample group-level analyses between whole brain correlation maps generated from the most anterior right hemisphere ROI (fourth column) and the precuneus ROI (fifth column). POS = parietal-occipital sulcus. See the online article for the color version of this figure.

significantly different regions of significantly different correlation (Figure 5C and 5D).

Seed-to-target rsFC analyses. Network-level analysis of each RS region ROI's connectivity fingerprint was conducted to evaluate whether individual ROIs possess distinguishable network membership profiles. All network nodes from a modified 17-network parcellation of Yeo et al. (2011) were used as targets for seed-to-target rsFC with each of the ipsilateral RS region ROIs. The 17-network parcellation was modified from the published version by first removing vertices for which there was low confidence in the assigned parcel membership (Yeo et al., 2011; Figure 6B, uncolored parcels) and then removing parcels in the general vicinity of the RS region that overlapped significantly with any of the seed ROIs (Figure 6B). This processing resulted in a 108 × 18 matrix representation of rsFC fingerprints for each subject, in which each row represents a different network node and each column a different RS region ROI (Figure 6A). Matrices were normalized with Fisher's r-to-z transformation prior to averaging and then converted back to Pearson correlations for presentation. Columns in Figure 6A are sorted according to the 17 Yeo et al. networks, and rows are sorted according to the hierarchical cluster analysis (HCA) displayed in Figure 6C.

Hierarchical cluster analysis. We performed an HCA on the seed-to-target network correlations in order to investigate how the seeds derived from the meta-analysis segregate based on connectivity. Each column of the group average 108 × 18 correlation matrix (Figure 6A; see Seed-Based rsFC Analyses) was treated as a vector in 108-dimensional space, and the Euclidean distance between each vector was calculated. Ward's linkage algorithm, which merges pairs of clusters that minimize the total sum of squares for the node to centroid distances, was applied to generate a cluster tree (Figure 6C). Because HCA will provide a clustering solution regardless of whether any true clusters exist, a bootstrapping procedure (Dosenbach et al., 2007) was used to validate the tree branch points. Low confidence values would suggest a random clustering of the data at each bootstrap, whereas high confidence values suggest the existence of true clusters in the data. A total of 5,000 bootstraps were generated by randomly sampling, with replacement, from the pool of HCP100 individual subject correlation matrices. The sampled matrices were averaged and clustered as above to create a set of 5,000 bootstrapped cluster trees. Confidence values at each branch point of the primary HCA were computed by calculating the proportion of bootstrap trees in which the subtree clustered the same seeds as the primary HCA.

Anatomical Mapping of the RSC

For clarity, we provide details describing the structure of the RS region, including descriptions of adjacent medial posterior brain regions that have been sometimes been included in definitions of the RSC. The human RSC has a diagonal orientation that shifts along its anterior-to-posterior extent, with the anterior RSC being the most dorsal. The most anterior part of the RSC is also the most medial and, moving posteriorly, the RSC extends laterally. Typically, medial areas of the RSC are also defined as anterior and superior, and lateral areas of the RSC are posterior and inferior. Connecting these terms with the neuroimaging studies included within the meta-analysis suggests that publications that refer to the RSC have included a number of regions outside of the anatomical RSC (Figure 1A). What we refer to as the *anterior RS region* relates to publications that have included the most posterior part of the posterior cingulate, the cingulate isthmus, and the anatomical RSC. Our definition of the *posterior RS region* includes portions of the parietal-occipital sulcus as well as some parts of the calcarine sulcus and lingual gyrus. The posterior RS region corresponds roughly to the functionally defined retrosplenial complex (Epstein, 2008). If an ROI was identified in an article by the authors as the RSC, or emerged as part of our meta-analysis, but contains only the calcarine and lingual gyrus, we refer to that region as *far posterior RS region*. When appropriate, we included both the anatomical (e.g., parietal-occipital sulcus) and functional (e.g., posterior RS region or RS complex) labels to facilitate this mapping across studies.

Results

Retrosplenial fMRI Meta-Analysis

Search results for the term *retrosplenial* in the Neurosynth database yielded 101 publications that used the term at least once in the article abstract. Refining the article metadata from these publications resulted in seven dominant cognitive domains associated with reported RS region recruitment: *emotion*, *imagery*, *learning*, *memory*, *navigation*, *scene processing*, and *vision*. Loading the publications associated with these domains into custom meta-analyses in Neurosynth revealed distinct and also overlapping RS subregions that mapped onto the different domains (Figure 2A-2B).

Memory mapped to the anterior and medial RS regions and showed a substantial bias for the left hemisphere. In contrast, *scene processing* and *navigation* showed a large degree of overlap within the POS—a region often reported as part of the retrosplenial *complex* in studies of navigation (Epstein, 2008). *Navigation* was diffusely localized, revealing nonoverlapping clusters within the lingual gyrus, superior RS region/precuneus, and anterior inferior RS region/PHC. *Imagery* showed a high degree of overlap with *navigation* and *scene processing* within the bilateral inferior POS and, additionally, portions of the *memory* region in the left hemisphere. The observation that *imagery* is so often reported as activating overlapping regions with *memory*, *scene*, and *navigation* suggests that mental imagery could be a common element of these processes. *Emotion* showed diffuse recruitment scattered across the entire region. *Learning* and *vision* revealed several small, nonunique clusters within the RS region, several of which did not survive ROI size exclusion thresholds (see Supplemental Figure 1 of the online supplemental materials).

Topic-Based Meta-Analytic Contrasts

To investigate cortical recruitment by the cognitive domains irrespective of "retrosplenial" as a search term, we refined the results of the meta-analysis by entering the domains into a "topic-based" meta-analysis in Neurosynth (Poldrack et al., 2012; Yarkoni et al., 2011). *Memory*, *scenes*, *navigation*, and *imagery* all demonstrated meta-analytic activation within the RS region from this topic-based search (see Supplemental Figure 3 of the online supplemental materials). *Memory* revealed activations throughout the RS region, particularly medially, whereas *navigation* and *scenes* recruitment primarily involved lateral RS regions. Activa-

tions for *imagery* were fairly evenly spread across the medial-lateral axis of the RS region. Mirroring the RS region-focused primary meta-analysis, *vision* and *learning* showed very little meta-analytic activation within the RS region. Interestingly, little to no *emotion* recruitment was seen within the RS region despite several clusters in the primary meta-analysis. However, the right lateral RS region was found to be recruited if we used a secondary *emotion* topic associated with *empathy* and *perspective-taking* (see Supplemental Figure 2 of the online supplemental materials).

Meta-analytic contrasts in Neurosynth between four primary domains of interest (*memory*, *scenes*, *navigation*, *imagery*) revealed several RS regions that were uniquely associated with one topic over the others. Left medial RS regions demonstrated a significantly stronger relationship to *memory* than to both *navigation* and *scenes* (Figure 2C), whereas no significant differences were found when contrasting *navigation* or *scenes* against *memory* in the RS region. The left RS region demonstrated an effect for *memory* over *emotion*. There were no significant differences between *scenes* and *navigation*, suggesting that the POS supports these functions similarly. There were no differences between *memory* and *imagery*, highlighting the strong cognitive and functional overlap between these two domains. In contrast, there were greater associations for *imagery* than for *navigation* in the left medial RS region (see Supplemental Figure 3 for all contrasts). Together, these findings suggest that the RS region supports multiple cognitive domains, with episodic memory and imagery functions primarily supported by left medial regions and scene processing and navigation functions primarily supported bilaterally in the POS.

MKDA Retrosplenial fMRI Meta-Analysis

The results from the MKDA meta-analysis (see Figure 3) largely mirrored those of the Neurosynth meta-analysis. Briefly, *memory* was the most widespread throughout the RS region, particularly along the midline, with somewhat more activation on the left hemisphere. *Navigation* and *scenes* showed a large degree of overlap, with *navigation* also more widespread and both extending into the POS and crossing into the occipital cortex. *Scenes* tended to be more lateral, with little midline activation, whereas *navigation* also included anterior areas. *Imagery* showed more midline and posterior activation. One difference between the manual and automated meta-analyses was the emergence of the term *self* in the manual meta-analysis in the left hemisphere, largely in the anterior and medial areas. We found little evidence for RS region recruitment for *vision* or *emotion*. Overall, the results from the manual meta-analysis largely support the conclusions of the automated meta-analysis.

Meta-Analytic Grid Search

A potential limitation of our meta-analysis approach is that it required the presence of the term *retrosplenial* in the title or abstract for a publication to be included. In order to capture all publications associated with this region, we inverted our meta-analysis approach to analyze changes in cognitive domain as a function of location. We conducted a generously defined grid search across the putative RS region using the "Locations" function in Neurosynth. Our search returned eight terms that met our selection criteria, which largely mirrored our findings from the other meta-analyses: *memory*, *navigation*, *scene*, *vision*, *self*, *emotion*, *imagery*, and also *theory of mind*—the only new term to emerge from this analysis.

Using *z*-score magnitude to establish winner-take-all domain membership revealed that *memory* appeared most frequently, located primarily in the medial RS region (Figure 4A). *Scenes* and *navigation* were localized more laterally, in addition to *vision*, which also extended inferior and posterior and was located outside the putative RS region within cuneus and lingual cortices. *Self* and *theory of mind* both appeared at superior points in grid space, approaching the precuneus. When taking into account overlap between domains, we found a high degree of overlap between *memory*, *navigation*, and *scenes*, such that approximately 24% of vertices that had loadings in the RS region were associated with some combination of the three terms; this overlap tended to be in the lateral RS region (Figure 4B; Supplemental Figure 4 of the online supplemental materials). We also found that *memory*, *self*, and *theory of mind* showed approximately 14% overlap overall, with the overlap located in the medial and superior section of the RS region, although *self* was more widespread than *theory of mind* (Figure 4C). Notably, *vision* was not typically associated with other terms. *Imagery* and *emotion* showed similar sparse conjunction with other domains (see Supplemental Figure 4). Together, these findings indicate that memory processes are ubiquitous throughout the RS region, and merge with *scene processing* and *navigation* processes in lateral/posterior RS regions, and with

Figure 6 (opposite). Node-by-network functional connectivity analysis and hierarchical cluster analysis. (A) regions of interest (ROIs) from the primary meta-analysis (horizontal axis of matrix; see Panel D, Figure 2, or Supplemental Figure 1 of the online supplemental materials) were used as seed regions for functional connectivity analyses with regions from the 17 networks from Yeo et al. (2011; vertical axis of matrix, networks separated by horizontal white lines) using the HCP100 (n = 100 participants) resting-state data. Normalized Pearson correlation values for each region with each cortical network are displayed in matrix format. Vertical white lines separate the three major divisions of the hierarchical clustering. Seeds are arranged in order based on their clustering in Panel C. Seed locations are shown in Panel D. (B) All parcels from a modified version of the Yeo et al. 17-network cortical parcellation were used as targets. Vertices with low confidence values were threshold out. Several targets with significant overlap with general retrosplenial cortex were also removed (black borders). (C) The group average correlation matrix was entered into a hierarchical clustering analysis to reveal associations between ROIs with closely related functional connectivity profiles. The seeds cluster into three separate branches segregated primarily by anatomical location, not cognitive domain. Confidence values (0 to 100) at each branch were established using a bootstrap procedure (1,000 iterations). (D) Seed ROIs used in the correlation analyses of Panels A and C for reference. Seed colors show cognitive domain, with additional anatomical label. VIS = visual network; SOMO = sensory motor network; DAN = dorsal attention network; VAN = ventral attention network; LIMB = limbic network; CCN = cognitive control network; DMN = default mode network; TP = temporal-parietal network. See the online article for the color version of this figure.

processes relating the *self* and others in medial/superior RS regions. These findings provide further evidence for dividing the RS region into subregions, while also highlighting *memory* as a potential unifying cognitive construct.

Resting State Functional Connectivity

The meta-analytic techniques utilized here sought to confirm the RS subregions that have been reported in the literature. We hypothesized that the functional connectivity profiles would provide additional insight into the diversity of subregions within the RS region. rsFC can add significant information that is useful for distinguishing brain subregions based on their locally varying connectivity fingerprints (e.g., Glasser et al., 2016). We used the locations resulting from the primary meta-analysis as seed regions for rsFC, excluding *learning* and *vision*, as described in the methods.

Figure 5 illustrates the capability of rsFC to divide ROIs associated with a single cognitive domain along their individual con-

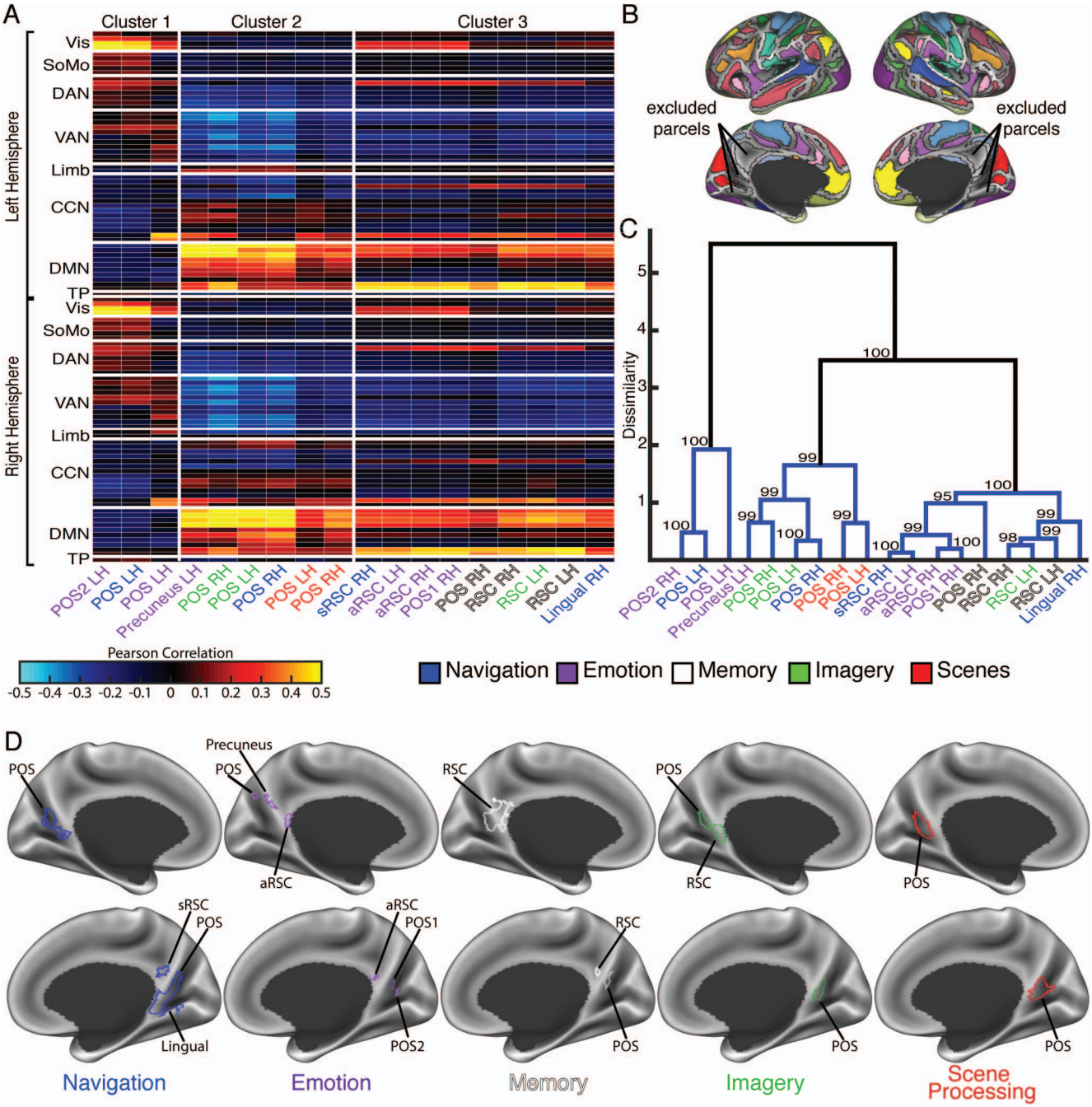

Figure 6 (opposite)

nectivity profiles. Each ROI (black outline) was associated with the *emotion*[1] meta-analysis. Seed-to-whole brain connectivity revealed different cortical (Figure 5A) and subcortical (Figure 5B) connectivity patterns for each ROI. Cuneal ROIs located just posterior to the POS displayed greater connectivity with the secondary visual cortex in the occipital lobe. Whole brain correlation maps generated by these cuneal ROIs were not significantly correlated with the other ipsilateral ROIs—indicating a transition to a different network at the POS. ROIs anterior and superior to the POS, on the edge of the putative RS region and precuneus, displayed significant connectivity with the canonical default mode network (DMN) regions (Raichle et al., 2001). ROIs in anterior RS regions also displayed strong connectivity to DMN regions, but the strengths of these connections varied in comparison. Thus, these results highlight the differential connectivity across the RS region. Furthermore, this finding illustrates that connectivity patterns do not necessarily reflect common task recruitment, as all seeds were derived from the same cognitive domain. Whole brain correlation maps generated from ROIs located in anterior RS regions were correlated with those generated by ROIs just posterior. A paired-sample group-level analysis for differences in the strength of connectivity found differential connectivity between each ipsilateral pair of ROIs (Figure 5C and 5D). The left hemisphere posterior ROI displayed stronger connectivity to DMN regions than the left hemisphere anterior RS region ROI (Figure 5C). However, in the right hemisphere, the anterior RS ROI demonstrated the stronger DMN connectivity (Figure 5D). These results further indicate the changing connectivity profiles between the POS, precuneus, and RSC proper.

Figure 6C illustrates the hierarchical clustering of seed regions from all cognitive domains, demonstrating the relationship between the cognitive domain, anatomical location, and connectivity fingerprint across the RS region. The hierarchical clustering analysis identified a split between the anterior and posterior RS regions, irrespective of task. The clusters also cut across functional domains, suggesting RS subregions that are recruited across multiple cognitive functions.

The rsFC results from ROIs derived from the *memory* cognitive domain meta-analysis show a strong resemblance to the canonical DMN typically derived from precuneus seeds placed superior to those used here (see Supplemental Figure 5 of the online supplemental materials). Included in this resemblance are anticorrelations between RS region *memory* seeds and the dorsal and ventral attention networks (VANs; Figure 6A). Figures 5 and 6A revealed that a large portion of the non-POS RS region is correlated with the DMN region; however, the meta-analytic contrast (see Meta-Analytic Contrasts results, Figure 2C) revealed that similar connectivity patterns do not necessarily equate to common task recruitment across the region. Finally, commonalities and differences in rsFC patterns between *imagery* and *navigation* again reveals the RS region as possessing subregions of unitary functional focus while sharing rsFC profiles (see Supplemental Figure 6 of the online supplemental materials).

Figure 6C presents the results of a hierarchical cluster analysis performed using the matrix presented in Figure 6A. The seeds were roughly divided once by the transition from the RSC proper into the POS and again by the banks of the POS, forming three stable clusters of regions among the set tested here, marked by white vertical lines in Figure 6A. Connectivity profiles of regions located rostral to the inferior/posterior bank of the POS (far posterior RS region) are dominated by visual connectivity. Seeds in both the RSC proper and within the POS both share the previously mentioned DMN connectivity but differ in their relative positive correlation to subnetworks within the DMN, relative positive correlation to dorsal attention network regions, and anticorrelation with VANs. For example, the seeds within the POS and posterior precuneus (mid/posterior RS region) have strong connectivity to intraparietal lobule, superior prefrontal cortex, medial prefrontal cortex, and lateral temporal lobe nodes of the DMN and have strong anticorrelations with the VAN. In contrast, seeds in anatomical RS cortex (anterior RS region) have stronger connectivity to the posterior intraparietal lobule and parahippocampal gyrus nodes of the DMN and demonstrate weaker anticorrelations with the VAN. Together with the meta-analytic results, these unsupervised clustering results provide converging evidence for the existence of RS subregions that share differing profiles of whole-brain network participation, including stark differences within the DMN.

Discussion

Here, we present evidence for functional diversity within the RS region using a combination of meta-analytic and rsFC techniques. We found functional subregions along the medial-lateral and anterior-posterior axes of the RS region. The novel combination of multiple large data sets leverages several streams of converging evidence for exploring cortical specialization.

Functional Diversity Within the Retrosplenial Cortex

Our results show that the POS—a region often reported as part of the retrosplenial *complex* (Epstein, 2008)—possesses task-based and rsFC profiles that differ from more anterior RS regions, consistent with recent work emphasizing the retinotopic organization of the inferior POS (Silson et al., 2016) and specialization across navigational tasks (Burles, Slone, & Iaria, 2017). The inferior POS is unique in that it can be well-defined with a functional localizer. Several studies have included the inferior POS as the *retrosplenial complex* (e.g., Baumann & Mattingley, 2010; Epstein, 2008; Marchette et al., 2014), which is confusing, as the label only includes a portion of the anatomical RSC. To reduce confusion, researchers should describe anatomical locations of activations in their studies, list peak coordinates from localizers, and include anatomical distinctions between the RSC proper and neighboring regions. Although we favor abandoning the term *retrosplenial complex* in favor of a label defined by its clear anatomical location (i.e., the inferior POS), our results highlight the existence of RS subregions and do support the use of functional localizers to differentiate the POS from surrounding medial cortex, including the RSC proper. Some recent publications, which are consistent with our findings, have side-stepped the issue of using RSC as a label by using the terms *posterior medial cortex* or *posterior midline regions* (e.g., Baldassano et al., 2017; Bird, Keidel, Ing, Horner, & Burgess, 2015; J. Chen et al., 2017).

[1] *Emotion* was selected as an illustrative example because of the relatively small seed sizes and wide distribution across the RSC. For this analysis, the location within the RSC was the primary factor of interest rather than the cognitive domain.

Although these articles were not included in the current grid search analysis, the results are consistent with our findings of anterior RS regions relating to mental imagery and could be incorporated into future meta-analyses using our grid search method.

We also observed differences between regional functional connectivity profiles in our rsFC analysis. Both anterior and medial RS regions and the more posterior POS connected to the DMN but differed in their connections with the dorsal-medial prefrontal cortex and medial temporal lobe subnetworks (Andrews-Hanna, Reidler, Sepulcre, Poulin, & Buckner, 2010; Braga & Buckner, 2017). In contrast, far posterior and lateral RS regions demonstrated functional connectivity with visual areas, similar to gradients observed in the precuneus (Peer, Salomon, Goldberg, Blanke, & Arzy, 2015) and the functionally defined parahippocampal place area (Baldassano, Beck, & Fei-Fei, 2013; Baldassano, Esteva, Fei-Fei, & Beck, 2016). A complementary gradient of both overlapping and distinct functions has been observed across the RS region and posterior cingulate when examining temporal aspects of network signaling (Mitra & Raichle, 2018), further supporting heterogeneity of function. In addition, the human posterior cingulate regions and the RSC differ in their correlations of resting glucose metabolism with other brain regions, further supporting the idea of differential functional connectivity across this region (Vogt, Vogt, & Laureys, 2006). Our functional connectivity results highlight diversity across the RS region as well as similarity within subregions of the RS region; strong rsFC differences were observed across the POS divide, but fairly similar profiles were found within anterior/medial RS regions (Figures 5 and 6).

These findings are supported by anatomical studies in animals, allowing for integration across structural and functional interpretations of RS cortex connectivity. Animal studies have shown variability in structural connectivity across the RSC (for review, see Miller, Vedder, Law, & Smith, 2014; Sugar, Witter, van Strien, & Cappaert, 2011), supporting the conclusion of functional subregions in the RS region. Both the granular and dysgranular anatomical RSC can be further divided into anterior and posterior sections, indicating the potential for functional diversity across the region (Vogt & Paxinos, 2014). Granular RSC—also referred to as BA29 and located in the anterior RSC—shares connections with the hippocampus, subiculum, and anterior thalamic nuclei (Kobayashi & Amaral, 2003, 2007; van Groen & Wyss, 1990), and BA29 head direction cells are sensitive to head direction alone (L. L. Chen, Lin, Green, Barnes, & McNaughton, 1994). In contrast, the more posterior and lateral dysgranular region of the RSC, or BA30, demonstrates connectivity with early visual areas, the parietal cortex, and the PHC (Kobayashi & Amaral, 2003, 2007; van Groen & Wyss, 1992), and has head direction cells that are sensitive to aspects of movement like speed or turns in addition to head direction (L. L. Chen et al., 1994). The dysgranular RSC also plays a role in associating local landmark cues with heading direction (Jacob et al., 2017), supporting a role in spatial and scene processing (e.g., Czajkowski et al., 2014; Hindley, Nelson, Aggleton, & Vann, 2014). The pattern of disruptions from rodent lesion studies suggests that the granular RSC is closely connected to limbic regions, whereas the dysgranular RSC is associated with neocortex (Miller et al., 2014). Anatomical connections in animals have been found between the RSC and the PHC, hippocampus, and medial prefrontal cortex (Kobayashi & Amaral, 2003, 2007; Sugar & Witter, 2016). A high density of reciprocal connections between the RSC and medial parietal cortex provides anatomical evidence that the RSC serves as the intermediary for information from parietal to medial temporal lobe regions, especially via the dysgranular RSC (Wilber et al., 2015). Thus, functionally, the RS region is an epicenter of information from vision, self-motion, and peri-personal space, and is ideally situated to synthesize information from these sources. Together, the anatomical and functional differences observed in animal studies suggests that the anterior (granular) RSC is associated with limbic and memory circuits and functions, whereas the posterior (dysgranular) RSC is associated with neocortical processing of visual and spatial information. These animal findings square nicely with the results of our meta-analyses and cluster analysis.

Commonalities in Function Across the Retrosplenial Cortex

Although our findings support the idea of functionally diverse subregions within the RS region, the results also point to commonalities that span across the entire RS region. One strong commonality is the ubiquity of memory processes throughout the RS region; both the general topic-based search (Supplemental Figure 2) and the grid search across the RS region (see Figure 4) support this finding. Although our primary meta-analysis found that *memory* was generally localized to the medial left hemisphere (see Figure 2), it is possible that those studies focused primarily on episodic memory while the more lateral regions show domain-specific memory for scenes and locations. In addition, it has been suggested that the RS region has a greater relationship with memory functions than do other scene areas (Baldassano et al., 2016; Silson et al., 2016); our approach highlights the important link between memory and multiple cognitive domains in the RS region.

Our results also support RS region involvement in visualizing oneself in the first-person from the perspective of other locations, time points, or people. The two primary divisions observed in the grid search space analysis (see Figure 4)—*navigation/scenes* and *self/theory of mind*—were spatially distinct from each other but included a large degree of overlap with *memory*. These findings suggest that the RS region could broadly support mentally projecting oneself into a different perspective. This unifying concept of self-referential spatiotemporal processing is supported by previous studies (see Chrastil, 2018, for review), including a link between social skills and spatial perspective-taking (Shelton, Clements-Stephens, Lam, Pak, & Murray, 2012), and studies demonstrating self-referential processing in midline regions of the brain (Andrews-Hanna, Saxe, & Yarkoni, 2014; Guterstam, Björnsdotter, Gentile, & Ehrsson, 2015; Leech & Sharp, 2014; Peer et al., 2015; Spreng, Mar, & Kim, 2009; Summerfield et al., 2009), with an overlap of spatial and temporal processing in RS regions (Gauthier & van Wassenhove, 2016). Additional research is needed to fully test whether the RS region supports this broader function; however, our results suggest that the RS region sits at a unique confluence of connectivity and function that could support the necessary computations for self-referential spatiotemporal processing.

Self-referential processing is consistent with other models of the RS region. For example, the RS region could translate between allocentric and egocentric perspectives (Byrne, Becker, & Burgess, 2007), as supported by animal work showing that the RSC is

sensitive to multiple reference frames and scales (Alexander & Nitz, 2015, 2017). Our findings broaden this model from a purely spatial projection to include temporal and social processing (i.e., emotion, self and theory of mind, future projection). Interestingly, BA30 of the RSC projects more heavily to posterior parietal cortex than the other way around (Olsen, Ohara, Iijima, & Witter, 2017), suggesting potential asymmetries in this translation that should be explored in future tests. Interestingly, the RS region is a key component of the DMN, and models of the DMN have focused on self-projection (Buckner & Carroll, 2007). The nearby posterior cingulate cortex, another node of the DMN, is also important for internally driven processing and demonstrates a gradient related to different cognitive processes, including self-reflection (Bzdok et al., 2015; Leech & Sharp, 2014; Vogt & Laureys, 2005), suggesting a similar role for the RS region. Our findings fit within the DMN framework but also demonstrate how self-projection processes differ across the RS region and expand self-projection into POS regions that are not typically considered part of the DMN.

Challenges for the Future

Our approach uses relatively unbiased methods, but there are some limitations to these techniques (Carter & McCullough, 2014; van Elk et al., 2015; Yarkoni et al., 2011). Our study was designed to investigate specific hypotheses about the function of the RS region, and our results suggest that incorporation of anatomical, functional, and connectivity methods may be the most comprehensive approach to studying this region. In the future, incorporating functional recruitment from multiple tasks and/or meta-analytic activation into the unsupervised clustering approach we used with rsFC could further identify neighboring RS regions. Our findings support the findings of a recent multimodal parcellation (MMP) of the cerebral cortex (Glasser et al., 2016), including the RSC, suggesting a convergence between methodologies. However, significant differences between the MMP and our results in anterior RS regions remain to be reconciled.

Finally, it is important to note that functional recruitment of the hippocampus and other brain regions are often reported in the same publications and same types of processing as those observed for the RS region. For example, temporal coordination of neural signals between the RSC and both the hippocampus and thalamus has been observed in rodents (Alexander et al., 2018; Bruna Del Vechio et al., 2017; Corcoran, Frick, Radulovic, & Kay, 2016; Young & McNaughton, 2009), suggesting a strong link between these regions. Interestingly, inference maps on the term *retrosplenial* in Neurosynth yielded activations in the PHC, hippocampus, precuneus, angular gyrus, and medial prefrontal cortex—all nodes of the canonical DMN—suggesting a high degree of coactivation between other DMN regions and the RS region. This finding highlights the difficulty in separating function specific to the RS region from that of the rest of the network (see Ekstrom, Arnold, & Iaria, 2014, for additional discussion of network interactions involving the RS region). Yet the differences we found in function and connectivity for RS subregions as they relate to DMN subnetworks could lead to specific predictions for individual cognitive domains that need to be tested functionally, both within the RS region and throughout the DMN. For example, compared with other components of the DMN, the RS region has increased connections to visual and parietal cortices (Villena-Gonzalez et al., 2018), suggesting a connectional difference from other DMN nodes. The relationship between the meta-analyses/rsFC-analyses shown here, network analysis, and empirical work spanning across cognitive domains presents the next major challenge and opportunity to understanding retrosplenial function.

In sum, we used an unbiased, data-driven approach to determine RS region function, which we anticipated could provide a blueprint for examining similar questions in other brain regions. We found strong evidence for functional heterogeneity across RS subregions. The subdivisions we derived should serve as targets for future studies, potentially benefitting both neuroimaging and clinical communities.

References

Alexander, A. S., & Nitz, D. A. (2015). Retrosplenial cortex maps the conjunction of internal and external spaces. *Nature Neuroscience, 18,* 1143–1151. http://dx.doi.org/10.1038/nn.4058

Alexander, A. S., & Nitz, D. A. (2017). Spatially periodic activation patterns of retrosplenial cortex encode route sub-spaces and distance traveled. *Current Biology, 27,* 1551–1560.e4. http://dx.doi.org/10.1016/j.cub.2017.04.036

Alexander, A. S., Rangel, L. M., Tingley, D., & Nitz, D. A. (2018). Neurophysiological signatures of temporal coordination between retrosplenial cortex and the hippocampal formation. *Behavioral Neuroscience, 132,* 453–468. http://dx.doi.org/10.1037/bne0000254

Amunts, K., Schleicher, A., & Zilles, K. (2007). Cytoarchitecture of the cerebral cortex—More than localization. *NeuroImage, 37,* 1061–1065.

Andrews-Hanna, J. R., Reidler, J. S., Sepulcre, J., Poulin, R., & Buckner, R. L. (2010). Functional-anatomic fractionation of the brain's default network. *Neuron, 65,* 550–562. http://dx.doi.org/10.1016/j.neuron.2010.02.005

Andrews-Hanna, J. R., Saxe, R., & Yarkoni, T. (2014). Contributions of episodic retrieval and mentalizing to autobiographical thought: Evidence from functional neuroimaging, resting-state connectivity, and fMRI meta-analyses. *NeuroImage, 91,* 324–335. http://dx.doi.org/10.1016/j.neuroimage.2014.01.032

Auger, S. D., Mullally, S. L., & Maguire, E. A. (2012). Retrosplenial cortex codes for permanent landmarks. *PLoS ONE, 7*(8), e43620. http://dx.doi.org/10.1371/journal.pone.0043620

Baldassano, C., Beck, D. M., & Fei-Fei, L. (2013). Differential connectivity within the parahippocampal place area. *NeuroImage, 75,* 228–237. http://dx.doi.org/10.1016/j.neuroimage.2013.02.073

Baldassano, C., Chen, J., Zadbood, A., Pillow, J. W., Hasson, U., & Norman, K. A. (2017). Discovering event structure in continuous narrative perception and memory. *Neuron, 95,* 709–721.e5. http://dx.doi.org/10.1016/j.neuron.2017.06.041

Baldassano, C., Esteva, A., Fei-Fei, L., & Beck, D. M. (2016). Two distinct scene-processing networks connecting vision and memory. *eNeuro, 3,* 057406. http://dx.doi.org/10.1523/ENEURO.0178-16.2016

Barch, D. M., Burgess, G. C., Harms, M. P., Petersen, S. E., Schlaggar, B. L., Corbetta, M., . . . WU-Minn HCP Consortium. (2013). Function in the human connectome: Task-fMRI and individual differences in behavior. *NeuroImage, 80,* 169–189. http://dx.doi.org/10.1016/j.neuroimage.2013.05.033

Baumann, O., & Mattingley, J. B. (2010). Medial parietal cortex encodes perceived heading direction in humans. *The Journal of Neuroscience, 30,* 12897–12901. http://dx.doi.org/10.1523/JNEUROSCI.3077-10.2010

Bird, C. M., Keidel, J. L., Ing, L. P., Horner, A. J., & Burgess, N. (2015). Consolidation of complex events via reinstatement in posterior cingulate cortex. *The Journal of Neuroscience, 35,* 14426–14434. http://dx.doi.org/10.1523/JNEUROSCI.1774-15.2015

Boccia, M., Piccardi, L., Palermo, L., Nemmi, F., Sulpizio, V., Galati, G., & Guariglia, C. (2015). A penny for your thoughts! patterns of fMRI

activity reveal the content and the spatial topography of visual mental images. *Human Brain Mapping, 36,* 945–958. http://dx.doi.org/10.1002/hbm.22678

Braga, R. M., & Buckner, R. L. (2017). Parallel interdigitated distributed networks within the individual estimated by intrinsic functional connectivity. *Neuron, 95,* 457–471.e5. http://dx.doi.org/10.1016/j.neuron.2017.06.038

Bruna Del Vechio, K., Kelly Soares, F., Francesca, B., Daniel, A.-F., Paul-Antoine, L., Alix, T.-C., . . . Claudio Marcos, Q. (2017). Electrophysiological evidence that the retrosplenial cortex displays a strong and specific activation phased with hippocampal theta during paradoxical (REM) sleep. *The Journal of Neuroscience, 37,* 8003–8013. http://dx.doi.org/10.1523/JNEUROSCI.0026-17.2017

Buckner, R. L., & Carroll, D. C. (2007). self-projection and the brain. *Trends in Cognitive Sciences, 11,* 49–57. http://dx.doi.org/10.1016/j.tics.2006.11.004

Burgess, G. C., Kandala, S., Nolan, D., Laumann, T. O., Power, J. D., Adeyemo, B., . . . March, D. M. (2016). Evaluation of denoising strategies to address motion-correlated artifacts in resting-state functional magnetic resonance imaging data from the human connectome project. *Brain Connectivity, 6,* 669–680.

Burles, F., Slone, E., & Iaria, G. (2017). Dorso-medial and ventro-lateral functional specialization of the human retrosplenial complex in spatial updating and orienting. *Brain Structure & Function, 222,* 1481–1493. http://dx.doi.org/10.1007/s00429-016-1288-8

Byrne, P., Becker, S., & Burgess, N. (2007). Remembering the past and imagining the future: A neural model of spatial memory and imagery. *Psychological Review, 114,* 340–375. http://dx.doi.org/10.1037/0033-295X.114.2.340

Bzdok, D., Heeger, A., Langner, R., Laird, A. R., Fox, P. T., Palomero-Gallagher, N., . . . Eickhoff, S. B. (2015). Subspecialization in the human posterior medial cortex. *NeuroImage, 106,* 55–71. http://dx.doi.org/10.1016/j.neuroimage.2014.11.009

Carter, E. C., & McCullough, M. E. (2014). Publication bias and the limited strength model of self-control: Has the evidence for ego depletion been overestimated? *Frontiers in Psychology, 5,* 823. http://dx.doi.org/10.3389/fpsyg.2014.00823

Chen, J., Leong, Y. C., Honey, C. J., Yong, C. H., Norman, K. A., & Hasson, U. (2017). Shared memories reveal shared structure in neural activity across individuals. *Nature Neuroscience, 20,* 115–125. http://dx.doi.org/10.1038/nn.4450

Chen, L. L., Lin, L. H., Green, E. J., Barnes, C. A., & McNaughton, B. L. (1994). Head-direction cells in the rat posterior cortex. I. Anatomical distribution and behavioral modulation. *Experimental Brain Research, 101,* 8–23. http://dx.doi.org/10.1007/BF00243212

Chrastil, E. R. (2018). Heterogeneity in human retrosplenial cortex: A review of function and connectivity. *Behavioral Neuroscience, 132,* 317–338. http://dx.doi.org/10.1037/bne0000261

Chrastil, E. R., Sherrill, K. R., Hasselmo, M. E., & Stern, C. E. (2015). There and back again: Hippocampus and retrosplenial cortex track homing distance during human path integration. *The Journal of Neuroscience, 35,* 15442–15452. http://dx.doi.org/10.1523/JNEUROSCI.1209-15.2015

Corcoran, K. A., Frick, B. J., Radulovic, J., & Kay, L. M. (2016). Analysis of coherent activity between retrosplenial cortex, hippocampus, thalamus, and anterior cingulate cortex during retrieval of recent and remote context fear memory. *Neurobiology of learning and memory, 127,* 93–101. http://dx.doi.org/10.1016/j.nlm.2015.11.019

Czajkowski, R., Jayaprakash, B., Wiltgen, B., Rogerson, T., Guzman-Karlsson, M. C., Barth, A. L., . . . Silva, A. J. (2014). Encoding and storage of spatial information in the retrosplenial cortex. *Proceedings of the National Academy of Sciences of the United States of America, 111,* 8661–8666. http://dx.doi.org/10.1073/pnas.1313222111

Dosenbach, N. U. F., Fair, D. A., Miezin, F. M., Cohen, A. L., Wenger, K. K., Dosenbach, R. A. T., . . . Petersen, S. E. (2007). Distinct brain networks for adaptive and stable task control in humans. *Proceedings of the National Academy of Sciences of the United States of America, 104,* 11073–11078. http://dx.doi.org/10.1073/pnas.0704320104

Ekstrom, A. D., Arnold, A. E. G. F., & Iaria, G. (2014). A critical review of the allocentric spatial representation and its neural underpinnings: Toward a network-based perspective. *Frontiers in Human Neuroscience, 8,* 803. http://dx.doi.org/10.3389/fnhum.2014.00803

Epstein, R. A. (2008). Parahippocampal and retrosplenial contributions to human spatial navigation. *Trends in Cognitive Sciences, 12,* 388–396. http://dx.doi.org/10.1016/j.tics.2008.07.004

Epstein, R. A., & Higgins, J. S. (2007). Differential parahippocampal and retrosplenial involvement in three types of visual *scene* recognition. *Cerebral Cortex, 17,* 1680–1693. http://dx.doi.org/10.1093/cercor/bhl079

Epstein, R., & Kanwisher, N. (1998). A cortical representation of the local visual environment. *Nature, 392,* 598–601. http://dx.doi.org/10.1038/33402

Fischl, B., Rajendran, N., Busa, E., Augustinack, J., Hinds, O., Yeo, B. T. T., . . . Zilles, K. (2008). Cortical folding patterns and predicting cytoarchitecture. *Cerebral Cortex, 18,* 1973–1980. http://dx.doi.org/10.1093/cercor/bhm225

Gauthier, B., & van Wassenhove, V. (2016). Time is not space: Core computations and domain-specific networks for mental travels. *The Journal of Neuroscience, 36,* 11891–11903. http://dx.doi.org/10.1523/JNEUROSCI.1400-16.2016

Glasser, M. F., Coalson, T. S., Robinson, E. C., Hacker, C. D., Harwell, J., Yacoub, E., . . . Van Essen, D. C. (2016). A multi-modal parcellation of human cerebral cortex. *Nature, 536,* 171–178. http://dx.doi.org/10.1038/nature18933

Glasser, M. F., Sotiropoulos, S. N., Wilson, J. A., Coalson, T. S., Fischl, B., Andersson, J. L., . . . WU-Minn HCP Consortium. (2013). The minimal preprocessing pipelines for the Human Connectome Project. *NeuroImage, 80,* 105–124. http://dx.doi.org/10.1016/j.neuroimage.2013.04.127

Griffanti, L., Salimi-Khorshidi, G., Beckmann, C. F., Auerbach, E. J., Douaud, G., Sexton, C. E., . . . Smith, S. M. (2014). ICA-based artefact removal and accelerated fMRI acquisition for improved resting state network imaging. *NeuroImage, 95,* 232–247. http://dx.doi.org/10.1016/j.neuroimage.2014.03.034

Guterstam, A., Björnsdotter, M., Gentile, G., & Ehrsson, H. H. (2015). Posterior cingulate cortex integrates the senses of self-location and body ownership. *Current Biology, 25,* 1416–1425. http://dx.doi.org/10.1016/j.cub.2015.03.059

Hindley, E. L., Nelson, A. J. D., Aggleton, J. P., & Vann, S. D. (2014). The rat retrosplenial cortex is required when visual cues are used flexibly to determine location. *Behavioural Brain Research, 263,* 98–107. http://dx.doi.org/10.1016/j.bbr.2014.01.028

Jacob, P.-Y., Casali, G., Spieser, L., Page, H., Overington, D., & Jeffery, K. (2017). An independent, landmark-dominated head-direction signal in dysgranular retrosplenial cortex. *Nature Neuroscience, 20,* 173–175. http://dx.doi.org/10.1038/nn.4465

Kobayashi, Y., & Amaral, D. G. (2000). Macaque monkey retrosplenial cortex: I. three-dimensional and cytoarchitectonic organization. *The Journal of Comparative Neurology, 426,* 339–365. http://dx.doi.org/10.1002/1096-9861(20001023)426:3<339::AID-CNE1>3.0.CO;2-8

Kobayashi, Y., & Amaral, D. G. (2003). Macaque monkey retrosplenial cortex: II. Cortical afferents. *The Journal of Comparative Neurology, 466,* 48–79. http://dx.doi.org/10.1002/cne.10883

Kobayashi, Y., & Amaral, D. G. (2007). Macaque monkey retrosplenial cortex: III. Cortical efferents. *The Journal of Comparative Neurology, 502,* 810–833. http://dx.doi.org/10.1002/cne.21346

Kucyi, A., Moayedi, M., Weissman-Fogel, I., Goldberg, M. B., Freeman, B. V., Tenenbaum, H. C., & Davis, K. D. (2014). Enhanced medial

prefrontal-default mode network functional connectivity in chronic pain and its association with pain rumination. *The Journal of Neuroscience, 34,* 3969–3975. http://dx.doi.org/10.1523/JNEUROSCI.5055-13.2014

Leech, R., & Sharp, D. J. (2014). The role of the posterior cingulate cortex in cognition and disease. *Brain: A Journal of Neurology, 137,* 12–32. http://dx.doi.org/10.1093/brain/awt162

Luo, Y., Huang, X., Yang, Z., Li, B., Liu, J., & Wei, D. (2014). Regional homogeneity of intrinsic brain activity in happy and unhappy individuals. *PLoS ONE, 9*(1), e85181. http://dx.doi.org/10.1371/journal.pone.0085181

Marchette, S. A., Vass, L. K., Ryan, J., & Epstein, R. A. (2014). Anchoring the neural compass: Coding of local spatial reference frames in human medial parietal lobe. *Nature Neuroscience, 17,* 1598–1606. http://dx.doi.org/10.1038/nn.3834

Miller, A. M. P., Vedder, L. C., Law, L. M., & Smith, D. M. (2014). Cues, context, and long-term memory: The role of the retrosplenial cortex in spatial cognition. *Frontiers in Human Neuroscience, 8,* 586. http://dx.doi.org/10.3389/fnhum.2014.00586

Mitra, A., & Raichle, M. E. (2018). Principles of cross-network communication in human resting state fMRI. *Scandinavian Journal of Psychology, 59,* 83–90. http://dx.doi.org/10.1111/sjop.12422

Olsen, G. M., Ohara, S., Iijima, T., & Witter, M. P. (2017). Parahippocampal and retrosplenial connections of rat posterior parietal cortex. *Hippocampus, 27,* 335–358. http://dx.doi.org/10.1002/hipo.22701

Park, S., & Chun, M. M. (2009). Different roles of the parahippocampal place area (PPA) and retrosplenial cortex (RSC) in panoramic scene perception. *NeuroImage, 47,* 1747–1756. http://dx.doi.org/10.1016/j.neuroimage.2009.04.058

Park, S., Intraub, H., Yi, D.-J., Widders, D., & Chun, M. M. (2007). Beyond the edges of a view: Boundary extension in human scene-selective visual cortex. *Neuron, 54,* 335–342. http://dx.doi.org/10.1016/j.neuron.2007.04.006

Peer, M., Salomon, R., Goldberg, I., Blanke, O., & Arzy, S. (2015). Brain system for mental orientation in space, time, and person. *Proceedings of the National Academy of Sciences of the United States of America, 112,* 11072–11077. http://dx.doi.org/10.1073/pnas.1504242112

Poldrack, R. A., Mumford, J. A., Schonberg, T., Kalar, D., Barman, B., & Yarkoni, T. (2012). Discovering relations between mind, brain, and mental disorders using topic mapping. *PLoS Computational Biology, 8*(10), e1002707. http://dx.doi.org/10.1371/journal.pcbi.1002707

Pothuizen, H. H. J., Davies, M., Albasser, M. M., Aggleton, J. P., & Vann, S. D. (2009). Granular and dysgranular retrosplenial cortices provide qualitatively different contributions to spatial working memory: Evidence from immediate-early gene imaging in rats. *European Journal of Neuroscience, 30,* 877–888. http://dx.doi.org/10.1111/j.1460-9568.2009.06881.x

Power, J. D., Mitra, A., Laumann, T. O., Snyder, A. Z., Schlaggar, B. L., & Petersen, S. E. (2014). Methods to detect, characterize, and remove motion artifact in resting state fMRI. *NeuroImage, 84,* 320–341. http://dx.doi.org/10.1016/j.neuroimage.2013.08.048

Pruessner, J. C., Köhler, S., Crane, J., Pruessner, M., Lord, C., Byrne, A., . . . Evans, A. C. (2002). Volumetry of temporopolar, perirhinal, entorhinal and parahippocampal cortex from high-resolution MR images: Considering the variability of the collateral sulcus. *Cerebral Cortex, 12,* 1342–1353. http://dx.doi.org/10.1093/cercor/12.12.1342

Raichle, M. E., MacLeod, A. M., Snyder, A. Z., Powers, W. J., Gusnard, D. A., & Shulman, G. L. (2001). A default mode of brain function. *Proceedings of the National Academy of Sciences of the United States of America, 98,* 676–682. http://dx.doi.org/10.1073/pnas.98.2.676

Robinson, E. C., Jbabdi, S., Glasser, M. F., Andersson, J., Burgess, G. C., Harms, M. P., . . . Jenkinson, M. (2014). MSM: A new flexible framework for Multimodal Surface Matching. *NeuroImage, 100,* 414–426.

Salimi-Khorshidi, G., Douaud, G., Beckmann, C. F., Glasser, M. F., Griffanti, L., & Smith, S. M. (2014). Automatic denoising of functional MRI data: Combining independent component analysis and hierarchical fusion of classifiers. *NeuroImage, 90,* 449–468. http://dx.doi.org/10.1016/j.neuroimage.2013.11.046

Shelton, A. L., Clements-Stephens, A. M., Lam, W. Y., Pak, D. M., & Murray, A. J. (2012). Should social savvy equal good spatial skills? The interaction of social skills with spatial perspective taking. *Journal of Experimental Psychology: General, 141,* 199–205. http://dx.doi.org/10.1037/a0024617

Sherrill, K. R., Erdem, U. M., Ross, R. S., Brown, T. I., Hasselmo, M. E., & Stern, C. E. (2013). Hippocampus and retrosplenial cortex combine path integration signals for successful navigation. *The Journal of Neuroscience, 33,* 19304–19313. http://dx.doi.org/10.1523/JNEUROSCI.1825-13.2013

Shine, J. P., Valdés-Herrera, J. P., Hegarty, M., & Wolbers, T. (2016). The human retrosplenial cortex and thalamus code head direction in a global reference frame. *The Journal of Neuroscience, 36,* 6371–6381. http://dx.doi.org/10.1523/JNEUROSCI.1268-15.2016

Silson, E. H., Steel, A. D., & Baker, C. I. (2016). Scene-selectivity and retinotopy in medial parietal cortex. *Frontiers in Human Neuroscience, 10,* 412. http://dx.doi.org/10.3389/fnhum.2016.00412

Smith, S. M., Beckmann, C. F., Andersson, J., Auerbach, E. J., Bijsterbosch, J., Douaud, G., . . . WU-Minn HCP Consortium. (2013). Resting-state fMRI in the Human Connectome Project. *NeuroImage, 80,* 144–168. http://dx.doi.org/10.1016/j.neuroimage.2013.05.039

Sotiropoulos, S. N., Jbabdi, S., Xu, J., Andersson, J. L., Moeller, S., Auerbach, E. J., . . . WU-Minn HCP Consortium. (2013). Advances in diffusion MRI acquisition and processing in the Human Connectome Project. *NeuroImage, 80,* 125–143. http://dx.doi.org/10.1016/j.neuroimage.2013.05.057

Spreng, R. N., Mar, R. A., & Kim, A. S. N. (2009). The common neural basis of autobiographical memory, prospection, navigation, theory of mind, and the default mode: A quantitative meta-analysis. *Journal of Cognitive Neuroscience, 21,* 489–510. http://dx.doi.org/10.1162/jocn.2008.21029

Steinvorth, S., Corkin, S., & Halgren, E. (2006). Ecphory of autobiographical memories: An fMRI study of recent and remote memory retrieval. *NeuroImage, 30,* 285–298. http://dx.doi.org/10.1016/j.neuroimage.2005.09.025

Sugar, J., & Witter, M. P. (2016). Postnatal development of retrosplenial projections to the parahippocampal region of the rat. *eLife, 5,* e13925. http://dx.doi.org/10.7554/eLife.13925

Sugar, J., Witter, M. P., van Strien, N. M., & Cappaert, N. L. M. (2011). The retrosplenial cortex: Intrinsic connectivity and connections with the (para)hippocampal region in the rat. An interactive connectome. *Frontiers in Neuroinformatics, 5,* 7. http://dx.doi.org/10.3389/fninf.2011.00007

Summerfield, J. J., Hassabis, D., & Maguire, E. A. (2009). Cortical midline involvement in autobiographical memory. *NeuroImage, 44,* 1188–1200. http://dx.doi.org/10.1016/j.neuroimage.2008.09.033

Summerfield, J. J., Hassabis, D., & Maguire, E. A. (2010). Differential engagement of brain regions within a "core" network during *scene* construction. *Neuropsychologia, 48,* 1501–1509. http://dx.doi.org/10.1016/j.neuropsychologia.2010.01.022

van Elk, M., Matzke, D., Gronau, Q. F., Guan, M., Vandekerckhove, J., & Wagenmakers, E.-J. (2015). Meta-analyses are no substitute for registered replications: A skeptical perspective on religious priming. *Frontiers in Psychology, 6,* 1365. http://dx.doi.org/10.3389/fpsyg.2015.01365

van Essen, D. C., Smith, S. M., Barch, D. M., Behrens, T. E. J., Yacoub, E., Ugurbil, K., & WU-Minn HCP Consortium. (2013). The WU-Minn Human Connectome Project: An overview. *NeuroImage, 80,* 62–79. http://dx.doi.org/10.1016/j.neuroimage.2013.05.041

Van Essen, D. C., Smith, J., Glasser, M. F., Elam, J., Donahue, C. J., Dierker, D. L., . . . Harwell, J. (2017). The Brain Analysis Library of Spatial maps and Atlases (BALSA) database. *NeuroImage, 144,* 270–274.

van Groen, T., & Wyss, J. M. (1990). Connections of the retrosplenial granular a cortex in the rat. *The Journal of Comparative Neurology, 300,* 593–606. http://dx.doi.org/10.1002/cne.903000412

van Groen, T., & Wyss, J. M. (1992). Connections of the retrosplenial dysgranular cortex in the rat. *The Journal of Comparative Neurology, 315,* 200–216. http://dx.doi.org/10.1002/cne.903150207

Vann, S. D., Aggleton, J. P., & Maguire, E. A. (2009). What does the retrosplenial cortex do? *Nature Reviews Neuroscience, 10,* 792–802. http://dx.doi.org/10.1038/nrn2733

Vass, L. K., & Epstein, R. A. (2013). Abstract representations of location and facing direction in the human brain. *The Journal of Neuroscience, 33,* 6133–6142. http://dx.doi.org/10.1523/JNEUROSCI.3873-12.2013

Villena-Gonzalez, M., Wang, H. T., Sormaz, M., Mollo, G., Margulies, D. S., Jefferies, E. A., & Smallwood, J. (2018). Individual variation in the propensity for prospective thought is associated with functional integration between visual and retrosplenial cortex. *Cortex: A Journal Devoted to the Study of the Nervous System and Behavior, 99,* 224–234. http://dx.doi.org/10.1016/j.cortex.2017.11.015

Vincent, J. L., Snyder, A. Z., Fox, M. D., Shannon, B. J., Andrews, J. R., Raichle, M. E., & Buckner, R. L. (2006). Coherent spontaneous activity identifies a hippocampal-parietal memory network. *Journal of Neurophysiology, 96,* 3517–3531. http://dx.doi.org/10.1152/jn.00048.2006

Vogt, B. A., & Laureys, S. (2005, January 1). Posterior cingulate, precuneal and retrosplenial cortices: Cytology and components of the neural network correlates of consciousness. *Progress in Brain Research, 150,* 205–207. http://dx.doi.org/10.1016/S0079-6123(05)50015-3

Vogt, B. A., & Paxinos, G. (2014). Cytoarchitecture of mouse and rat cingulate cortex with human homologies. *Brain Structure & Function, 219,* 185–192. http://dx.doi.org/10.1007/s00429-012-0493-3

Vogt, B. A., Vogt, L., & Laureys, S. (2006). Cytology and functionally correlated circuits of human posterior cingulate areas. *NeuroImage, 29,* 452–466. http://dx.doi.org/10.1016/j.neuroimage.2005.07.048

Vogt, B. A., Vogt, L. J., Perl, D. P., & Hof, P. R. (2001). Cytology of human caudomedial cingulate, retrosplenial, and caudal parahippocampal cortices. *The Journal of Comparative Neurology, 438,* 353–376. http://dx.doi.org/10.1002/cne.1320

Wager, T. D., Lindquist, M., & Kaplan, L. (2007). Meta-analysis of functional neuroimaging data: Current and future directions. *Social Cognitive and Affective Neuroscience, 2,* 150–158. http://dx.doi.org/10.1093/scan/nsm015

Wager, T. D., Lindquist, M. A., Nichols, T. E., Kober, H., & Van Snellenberg, J. X. (2009). Evaluating the consistency and specificity of neuroimaging data using meta-analysis. *NeuroImage, 45*(Suppl. 1), S210–S221. http://dx.doi.org/10.1016/j.neuroimage.2008.10.061

Wilber, A. A., Clark, B. J., Demecha, A. J., Mesina, L., Vos, J. M., & McNaughton, B. L. (2015). Cortical connectivity maps reveal anatomically distinct areas in the parietal cortex of the rat. *Frontiers in Neural Circuits, 8,* 146. http://dx.doi.org/10.3389/fncir.2014.00146

Winkler, A. M., Ridgway, G. R., Webster, M. A., Smith, S. M., & Nichols, T. E. (2014). Permutation inference for the general linear model. *NeuroImage, 92,* 381–397. http://dx.doi.org/10.1016/j.neuroimage.2014.01.060

Winkler, A. M., Webster, M. A., Vidaurre, D., Nichols, T. E., & Smith, S. M. (2015). Multi-level block permutation. *NeuroImage, 123,* 253–268. http://dx.doi.org/10.1016/j.neuroimage.2015.05.092

Wolbers, T., & Büchel, C. (2005). Dissociable retrosplenial and hippocampal contributions to successful formation of survey representations. *The Journal of Neuroscience, 25,* 3333–3340. http://dx.doi.org/10.1523/JNEUROSCI.4705-04.2005

Yarkoni, T., Poldrack, R. A., Nichols, T. E., Van Essen, D. C., & Wager, T. D. (2011). Large-scale automated synthesis of human functional neuroimaging data. *Nature Methods, 8,* 665–670. http://dx.doi.org/10.1038/nmeth.1635

Yeo, B. T. T., Krienen, F. M., Sepulcre, J., Sabuncu, M. R., Lashkari, D., Hollinshead, M., . . . Buckner, R. L. (2011). The organization of the human cerebral cortex estimated by intrinsic functional connectivity. *Journal of Neurophysiology, 106,* 1125–1165. http://dx.doi.org/10.1152/jn.00338.2011

Young, C. K., & McNaughton, N. (2009). Coupling of theta oscillations between anterior and posterior midline cortex and with the hippocampus in freely behaving rats. *Cerebral Cortex, 19,* 24–40. http://dx.doi.org/10.1093/cercor/bhn055

Received March 8, 2018
Revision received August 20, 2018
Accepted August 21, 2018 ■